The Fold and the Record

The Substrate Architecture of VERSF

Keith Taylor *VERSF Theoretical Physics Programme*

Abstract for the General Reader

Physicists routinely write equations describing electric and magnetic fields, the curvature of spacetime, and the flow of time. These equations are remarkably successful — they predict experiments with extraordinary accuracy. But they leave open a question that is rarely tackled head-on: *what is the physical substrate these descriptions are descriptions of?*

This paper, part of the VERSF research programme, proposes a single answer. Most of physics, at its deepest level, lives on a thin active **interface** — a structured layer separating two very different regimes of reality. On one side is the **Void** — pure possibility, with no facts, no shape, and no time. On the other side is the **committed world** — events that have happened irreversibly and cannot be undone. The interface is where folds form. A **fold** is the elementary unit of distinguishability — the first asymmetry from the void, a committed distinction that becomes part of the permanent record of what has happened.

The paper develops the consequences of placing physics on this interface. Electricity and magnetism turn out to be large-scale patterns in how the interface transports information. The familiar **gauge symmetry** of physics — usually treated as a mathematical convenience — emerges as the natural freedom to describe the same underlying transport in different local coordinates. Light, geometric structure, and even gravity all emerge from the same interface dynamics, at progressively coarser scales.

The picture is unusual but not vague. The paper specifies the interface's variables, its dynamics, and its topology, and shows how the standard equations of electromagnetism and gravity follow as large-scale approximations of more fundamental interface behaviour. It does not claim to derive all of physics from first principles. Its claim is more focused: that the things physics describes — fields, forces, spacetime, time itself — all live on a single physical layer, and that locating that layer matters.

Technical Abstract

Earlier papers in the VERSF programme established the *admissibility architecture* of the framework: finite distinguishability, irreversible commitment, the commitment interface, the formation of folds at that interface, and the emergence of effective continuum physics from the

operational reconstruction of a committed record. Those papers were structural. They asked what reality must satisfy in order for stable facts to exist.

The present paper asks a different question:

Where, physically, do the dynamical degrees of freedom of the framework reside?

The central proposal is that the physically active substrate of VERSF is **not the zero-entropy Void**, but the **closure-bearing commitment interface** that separates the reversible pre-commitment sector from the committed record sector. This interface is where distinguishability stabilises, where topology first becomes nontrivial, where folds — the first distinguishable asymmetries from the void — form, and where gauge transport dynamics emerge.

Four connected claims are developed.

1. **Gauge redundancy** is interface encoding degeneracy: locally distinct representations of the same closure transport.
2. **Electromagnetic transport** — Abelian and U(1)-type in the present treatment — is the continuum hydrodynamic limit of conserved closure transport on the interface.
3. **The K = 7 constraint dimensionality**, established in companion programme work, fixes the admissibility structure of the interface and forces hexagonal tiling with channel count $N\_\text{loop} = 14$.
4. **Spacetime geometry and gravity** emerge from the large-scale reconstruction of the accumulated committed record generated by interface dynamics.

These claims rest on an explicit interface substrate: discrete cells $\varphi_i = (\sigma_i, \omega_i)$ carrying orientation and closure-parity data, governed by a local transport action S_int combining nearest-neighbour transport, closure penalties, and commitment thresholds. Each cell of the interface carries the four-state Hilbert space $\mathscr{H}\_\text{fold} \cong \mathbb{C}^4$ of one fold, with the bridge between cell-level (σ, ω) labels and $\mathbb{C}^4$ basis states made explicit in §4.5. Non-Abelian generalisations of the closure structure are developed in two companion papers along independent routes.

Together these reframe VERSF as a theory of **interface physics**: a framework in which gauge structure, Maxwell transport, geometry, and gravitational response all emerge from the closure dynamics of a physically active commitment interface populated by folds.

Table of Contents

---

1. Introduction

The VERSF programme began from a foundational question:

What structural conditions must reality satisfy in order for stable physical facts to exist?

In answering this, the programme developed:

- **finite distinguishability** as the primitive that allows alternatives to be operationally separable;
- **irreversible commitment** as the mechanism by which alternatives become facts;
- **admissibility closure** as the constraint that selects physically realisable structures;
- the **commitment interface** separating reversible possibility from committed reality, on which folds form;
- the **fold** as the elementary unit of distinguishability — the first asymmetry from the void, a single committed distinction;
- the **committed record field** $\rho(x,t)$ as the accumulated trace of fold formation;
- and the **K = 7 constraint dimensionality** — the integer counting independent admissibility constraints — established by convergent argument across geometric, gauge-theoretic, topological, and combinatorial routes.

These structures were derived through admissibility arguments, closure theorems, topological constraints, and operational reconstruction principles. The resulting framework is *coherent at the level of structure*, but is largely silent on a more concrete physical question:

Where, in the substrate hierarchy, are the dynamical degrees of freedom of the framework physically located?

This paper proposes a direct answer:

The physically active substrate of VERSF is the commitment interface on which folds form.

The Void is not a bulk-field medium in the ordinary sense. It contains no committed distinctions, no stable topology, no entropy-bearing structure, and no operational geometry. The first physically meaningful structure of the programme appears at the interface on which reversible distinguishability becomes irreversible commitment. That interface is the locus on which folds — the first distinguishable asymmetries from the void — form, and it is the focus of the present paper.

Relation to the earlier transport programme

The present paper should be read as the **ontological and geometric continuation** of the earlier VERSF transport programme. Previous papers established the admissibility-theoretic reconstruction of Maxwell-form transport from Bit Conservation & Balance (BCB), Ticks-Per-Bit (TPB), gauge redundancy as informational degeneracy, and discrete substrate transport structures admitting continuum gauge limits. The purpose of the present paper is *not to rederive those transport results in full technical detail*, but to identify the physical locus at which those transport structures reside and acquire ontological meaning.

In this sense, the present work shifts the emphasis of the programme:

from admissible transport structure to interface-localised substrate physics.

The commitment interface is proposed as the physically active closure-bearing layer on which folds form and on which the transport structures developed in the earlier Maxwell admissibility programme become operationally realised.

Plan of the paper

§2 fixes the Void's status as a constraint medium without operational structure. §3 establishes the commitment interface as a physically active substrate on which folds form. §4 introduces the explicit interface variables and transport action on which the subsequent derivations rest, including (in §4.5) the bridge from the cell-level (σ, ω) structure to the per-fold $\mathbb{C}^4$ Hilbert space used in companion programme work. §5 develops the commitment dynamics that generate the record field. §6 derives gauge structure from interface encoding redundancy, formalised as Lemma 6.1. §7 derives Maxwell transport as the continuum hydrodynamic limit of conserved closure transport, formalised as Lemma 7.2, with a scope note identifying the U(1) emergence treated here as one channel of the broader SU(3) × SU(2) × U(1) structure developed in companion papers. §8 situates the K = 7 constraint dimensionality and the hexagonal tiling that supports the channel count $N\_{\text{loop}} = 14$. §§9–10 develop geometry and gravity as bulk reconstructions of the accumulated record, with explicit acknowledgement of the parallel causal-set treatment in the companion synthesis paper. §11 places the paper in interpretive context. §12 proposes a candidate VERSF master action unifying the substrate-structural development of §§3–10: §§12.1–12.5 state the programmatic structure (action, RG flow, fixed-point hierarchy, universality class, central conjecture); §§12.6–12.13 develop the first concrete computational instances (explicit block-fold RG flow, first-pass critical exponents, conservation-fixed closure-response kernel, constrained uniqueness of the local record-current functional, structural decomposition of SU(3) × SU(2) × U(1) from $\mathscr{H}\_{\text{fold}}$, Monte Carlo lattice programme, first preliminary numerical diagnostics); §12.14 collects the remaining open items. §13 closes with the ontological chain in summary form.

The structure of the argument can be summarised in a single figure.

Figure 1. The Ontological Chain

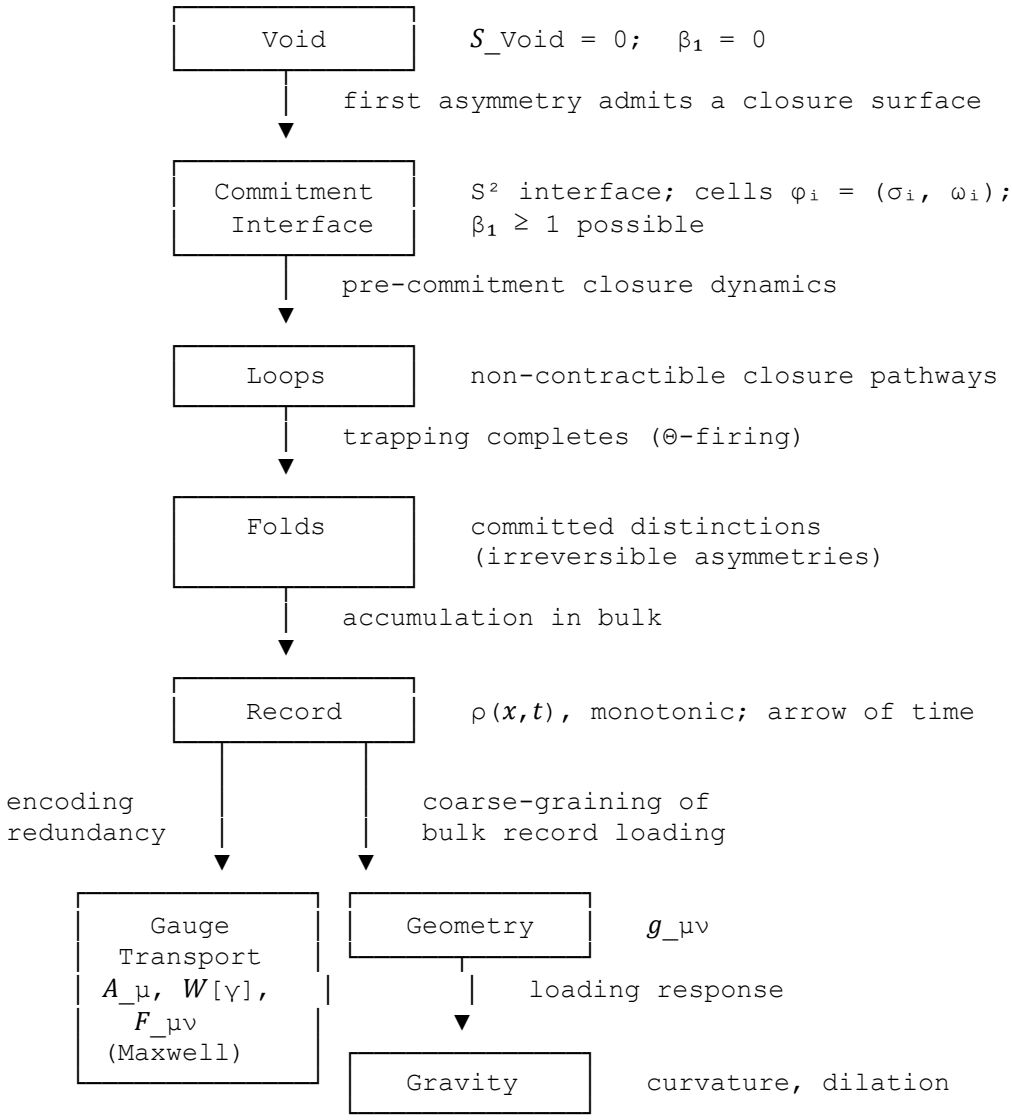

Each link of this chain is given a definite structural meaning in what follows.

---

2. The Void: A Constraint Medium without Operational Structure

The Void of VERSF is not ordinary vacuum.

Standard quantum vacuum already carries field structure, zero-point fluctuations, Hilbert-space organisation, and entropy capacity. The VERSF Void is a more primitive object: it is defined by the *absence* of:

- committed distinguishability,
- stable records,
- nontrivial topology,
- and any irreversible structure.

Hence

$S\_\text{Void} = 0$

not because the Void is empty matter but because **entropy itself requires distinguishability**. Without distinguishability there is no informational multiplicity, no stable alternatives, and no operationally definable physical entropy.

The Void therefore functions as a *constraint medium*: a capacity reservoir of unresolved possibility, modulated by — but not itself carrying — committed structure.

The central fact about the Void, for present purposes, is the following.

Proposition 2.1 (Void Looplessness). *The Void supports no stable closed loops.*

The argument is structural rather than dynamical. A stable loop requires distinguishable points along its path together with a stable identification of its endpoints. Both requirements presuppose committed distinguishability, which the Void by definition lacks. Equivalently, the first Betti number β_1 of the Void is zero, not as a contingent fact but as a defining condition.

This matters because in VERSF:

- **loops generate topology**;
- **topology permits trapping**;
- **trapping permits irreversible commitment**;
- **irreversible commitment produces folds — the elementary units of physical distinguishability**.

The first physically meaningful loops therefore cannot exist *inside* the Void. They must exist on the closure-bearing interface where committed distinguishability first appears — the interface at which folds form.

---

3. The Commitment Interface as Physical Substrate

The commitment interface is the closure-bearing 2-surface separating reversible possibility from irreversibly committed structure. It is the locus at which **folds** — committed distinctions, the first physically real asymmetries from the void — form. Earlier papers in the programme established three structural facts about this interface:

- it is the **minimal intrinsic commitment surface**;
- it is **topologically equivalent to S^2**, and more specifically two-dimensional (the dimensionality itself is derived in companion work — see below);
- it carries **binary geometric data** (σ, ω) at each cell, encoding orientation and closure parity for the fold formed at that cell.

The two-dimensional character of the interface receives two independent justifications in the programme, converging from opposite directions. Companion programme work on hexagonal interface light propagation shows that primitive D-dimensional fact-commitment fails for $D \geq 3$ under finite-budget admissibility: the distinguishability budget per addressable register dilutes as r^{−(D−2)} and falls below the per-fold commitment threshold at finite radius, placing $D = 2$ as the **maximal** admissible dimension. Independent companion programme work on the tick–bit asymmetry shows that $D = 2$ is also the **minimal** geometry capable of supporting irreversible distinguishability, requiring both (i) boundary capacity scaling as $|\partial R| = \Omega(\sqrt{|R|})$, absent in one-dimensional / constant-separator substrates, and (ii) generic local cycles enabling enclosure, absent in trees and branching graphs. The two routes converge: $D = 2$ is both maximal under budget admissibility and minimal under fact-localisation, and the interface inherits its dimensionality from both directions at once. The 2D character of the interface is therefore not itself emergent — it is the minimal substrate that any framework treating committed distinctions as physical primitives must adopt.

Terminological note. The companion programme work on bit formation analyses commitment events **informationally** as bit formation — each event collapses a many-to-one map and commits one classical bit. The present paper analyses the same events **topologically** as fold formation — each event is characterised by its (σ, ω) data and the local closure structure that supports it on the interface. A single fold carries one classical bit; the two terminologies pick out the same commitment event under its topological and informational aspects respectively, not the same object.

The present paper advances a stronger claim about the interface's status:

The commitment interface is proposed as the first physically active substrate layer of the VERSF framework.

It is the layer on which folds form, on which closure transport occurs, on which loops trap and complete, and from which the record accumulates. Concretely, the commitment interface simultaneously occupies four roles:

1. **Sectoral interface.** It separates the reversible pre-commitment sector from the committed sector.
2. **Transport substrate.** It carries the conserved closure currents whose continuum limit will be identified with Maxwell transport in §7.
3. **Topological support.** It is the lowest-level locus on which $\beta_1 \geq 1$ becomes possible, and therefore the locus where stable loops first exist.

4. **Fold-formation surface.** It is where reversible pre-commitment evolution terminates in irreversible fold formation — where the elementary units of physical distinguishability crystallise.

This four-role unification has immediate consequences. It explains why holographic behaviour, area scaling, Wilson loops, holonomies, and gauge redundancy recur naturally throughout the VERSF framework: the relevant physics does not initially live in the bulk Void, it lives on the closure interface, and interface-localised structure is precisely the kind of structure for which these phenomena are natural.

The (σ, ω) data is not a decorative addition. Orientation σ determines the *direction* of closure transport across the interface; closure parity ω determines whether a closure pathway can compose coherently with its neighbours. Both will reappear in §6 as the structural origin of gauge phase and gauge redundancy. The next section makes these variables, and their dynamics, fully explicit, and establishes the bridge to the per-fold four-dimensional complex Hilbert space $\mathscr{H}$_fold ≅ $\mathbb{C}^4$ used in the companion programme.

---

4. The Interface Lattice and Transport Action

The commitment interface has so far been described topologically (S^2 with (σ, ω) data) and dynamically (a substrate on which folds form). To pass from this conceptual description to a substrate physics from which the Maxwell transport and gauge structure of subsequent sections can be derived, we need explicit local variables and an explicit transport dynamics.

4.1 Interface cells

The commitment interface decomposes into discrete cells indexed by i. Each cell hosts one fold and carries a pair of binary geometric data,

$\varphi_i = (\sigma_i, \omega_i)$

where $\sigma_i \in \{\pm 1\}$ encodes local orientation and $\omega_i \in \{\pm 1\}$ encodes local closure parity. The pair $\varphi_i \in \mathbb{Z}_2 \times \mathbb{Z}_2$ is the **state of the fold at cell i**, and the configuration

$\{\varphi_i\} = \{(\sigma_i, \omega_i)\}_i$

is the **interface state** of the whole S^2 surface.

The following definition consolidates the substrate-level objects used throughout the rest of the paper:

Definition 4.1 (Interface state space). Let Σ be a compact two-dimensional commitment interface homeomorphic to S^2, tiled by hexagonal cells indexed by $i \in V$. Each cell carries a fold state

$\varphi_i = (\sigma_i, \omega_i) \in \mathbb{Z}_2 \times \mathbb{Z}_2$,

with associated per-fold Hilbert space $\mathscr{H}\_\text{fold} \cong \mathbb{C}^4$ (the cell↔$\mathbb{C}^4$ bridge is developed in §4.5). The total finite interface state space over a region $R \subset \Sigma$ is

$\mathscr{H}\_R = \bigotimes_{i \in R} \mathscr{H}\_\text{fold}$.

Cells are connected by oriented edges (links) $\langle ij \rangle$ carrying transport variables $U_{ij} \in U(1)$ (or, in non-Abelian completions, in a non-Abelian closure group), and loops ℓ on the cell complex carry loop holonomies $U\_\ell = \prod\_{\langle ij \rangle \in \ell} U_{ij}$.

The $\mathbb{Z}_2 \times \mathbb{Z}_2 \to \mathbb{C}^4$ bridge of §4.5 is now an explicit per-cell statement: each $(\sigma_i, \omega_i) \in \mathbb{Z}_2 \times \mathbb{Z}_2$ specifies one of four orthogonal basis states of $\mathscr{H}\_\text{fold} \cong \mathbb{C}^4$, and a configuration $\{\varphi_i\}$ over a region R specifies a product basis state of $\mathscr{H}\_R$.

4.2 Local update maps

Adjacent cells i and j (write $\langle ij \rangle$ for an adjacent pair) are related by local update maps

$U_{ij} : \varphi_i \mapsto \varphi_j$

which carry orientation and parity from one cell to the next. Two structural properties hold by construction:

- $U_{ji} = U_{ij}^{-1}$ — transport is locally invertible at the cell level;
- the composition of updates around a closed pathway γ on the interface defines a **closure operator**

  $U\_\gamma = \prod\_{\{\langle ij \rangle \in \gamma\}} U_{ij}$.

A pathway γ is **trivially consistent** when $U\_\gamma = \mathbb{1}$ (the identity) and **non-trivially consistent** when $U\_\gamma \neq \mathbb{1}$. The latter case generates holonomy.

4.3 Loop consistency constraints

For the interface to support stable physical transport, closure operators U_γ must satisfy **loop consistency**: the value of U_γ must depend only on the homotopy class of γ, not on its detailed path. Equivalently, infinitesimally contractible loops must close trivially:

$U\_\{\delta\gamma\} = \mathbb{1}$ for every contractible $\delta\gamma$.

This condition is what permits coarse-graining. It guarantees that local update structure on the cells aggregates coherently into transport at the continuum scale, and it is the structural origin of the Bianchi identity that will appear in §7.

4.4 The transport action

Closure dynamics on the interface is governed by a transport action of the form

$S\_\text{int} = \Sigma\_\{\langle ij\rangle\}\ \mathscr{A}(\varphi_i, \varphi_j) + \Sigma\_\{\ell\}\ \mathcal{C}\_\ell + \Sigma\_\{\ell\}\ \Theta(\mathcal{C}\_\ell - \mathcal{C}^*)$

where:

- $\mathscr{A}(\varphi_i, \varphi_j)$ is the **nearest-neighbour transport term**, penalising orientation/parity mismatches between adjacent cells and setting the cost of local closure transport;
- $\mathcal{C}\_\ell$ is the **closure penalty** for loop ℓ, enforcing loop consistency by suppressing configurations that fail the $U\_\{\delta\gamma\} = \mathbb{1}$ condition at contractible loops;
- $\Theta(\mathcal{C}\_\ell - \mathcal{C})^*$ is the **fold-formation threshold operator**: when the closure penalty on a loop ℓ exceeds a critical value $\mathcal{C}^*$, the loop transitions irreversibly into a committed configuration and a fold is formed. Below threshold, the dynamics on ℓ remain reversible; above threshold, the loop's closure structure is fixed and the resulting fold contributes to the record.

A minimal explicit realisation, supplied here as a concrete instance the reader can inspect rather than as the canonical form, takes $\mathscr{L}$ as a sum of Ising-type orientation and parity terms and $\mathcal{C}\_\ell$ as a Wilson-type closure penalty:

$S\_\text{int} = J\ \Sigma\_\{\langle ij\rangle\}\ (1 - \sigma_i\sigma_j) + K\ \Sigma\_\{\langle ij\rangle\}\ (1 - \omega_i\omega_j) + \lambda\ \Sigma\_\{\ell\}\ (1 - \mathrm{Re}\ U\_\ell) + \Sigma\_\{\ell\}\ \Theta(\mathcal{C}\_\ell - \mathcal{C}^*),$

with link variables $U_{ij} \in \mathrm{U}(1)$ and loop holonomies

$U\_\ell = \prod\_\{\langle ij\rangle \in \ell\}\ U_{ij}.$

This explicit form makes three structural features manifest: the orientation sector (J term) and parity sector (K term) act as independent Ising-type $\mathbb{Z}_2 \times \mathbb{Z}_2$ couplings consistent with Definition 4.1; the closure penalty (λ term) is the Wilson form familiar from lattice gauge theory; and the fold-formation threshold (Θ term) is a step function on the closure penalty itself. Couplings J, K, λ and the threshold $\mathcal{C}^*$ are substrate parameters of the framework, not adjustable phenomenological inputs.

The three terms have distinct physical roles. The first two set reversible pre-commitment dynamics: small fluctuations of σ_i and ω_i at fixed topology. The third enforces global coherence: the same configuration must produce the same closure operator regardless of path. The fourth governs the transition from reversible evolution to irreversible fold formation: the fold-formation threshold $\mathcal{C}^*$ is the operational locus at which β_1 jumps from 0 to ≥ 1 in the local closure complex, in the sense of Proposition 5.1 below.

The detailed forms of $\mathscr{L}$ and $\mathcal{C}\_\ell$ — and the precise value of $\mathcal{C}^*$ — are developed elsewhere in the programme. What matters for present purposes is the action's structural shape: it is local, nearest-neighbour, and supplemented by closure penalties and a fold-formation threshold. This is the discrete substrate dynamics from which the continuum Maxwell transport of §7 will emerge as a coarse-grained limit, and on which the gauge structure of §6 will be built.

The local, nearest-neighbour structure of $S_$int is reminiscent of lattice gauge theory in the Wilson–Kogut–Susskind tradition (Wilson, 1974; Kogut & Susskind, 1975), though the present construction is not a lattice approximation to a pre-existing continuum theory but a substrate dynamics in its own right.

4.5 From cells to $\mathbb{C}^4$: the per-fold Hilbert space

The cell-level structure $\varphi_i = (\sigma_i, \omega_i) \in \mathbb{Z}_2 \times \mathbb{Z}_2$ introduced in §4.1 is the discrete substrate at each cell of the interface. Each cell hosts a single fold, and the four possible (σ, ω) configurations of that cell are the four possible states of that fold. Subsequent VERSF derivations of gauge structure, particle content, and quantum correlations work in the four-dimensional complex Hilbert space $\mathscr{H}_$fold $\cong \mathbb{C}^4$ associated with one fold. These are not parallel structures but the same object at different scales.

The bridge is established along three independent routes in companion programme work. The first route derives $\mathscr{H}_$fold $\cong \mathbb{C}^4$ from the admissibility axioms A1–A3 by showing that the minimal commitment interface must be a two-dimensional surface carrying a four-dimensional complex state space per fold, with the complex structure itself derived (real spaces lack sufficient phase geometry to support interferometric distinguishability, in alignment with the experimental falsification of real-valued quantum theory in Renou et al., 2022; quaternionic spaces are non-minimal, doubling the state-space dimension without supplying new structural content, as discussed in the foundations of quaternionic quantum mechanics by Adler, 1995). A second route in the programme — derivation of fundamental physics from a single unit of distinguishability — independently establishes dim($\mathscr{H}_$fold) = 4 as the unique spectral attractor of the tick dynamics underlying the cell-level evolution: one bit (axiom A5) plus reversible directionality (axiom A2) plus orthogonality of distinguishable states forces exactly four basis states $|b, d\rangle$ with $b \in \{0, 1\}$, $d \in \{\pm 1\}$. A third route, from companion programme work on gravity from fold density gradients, arrives at the same dimension from a third angle: the minimum local Hilbert structure supporting exactly one irreducible binary outcome under irreversible dynamics requires four states — a two-dimensional amplitude sector (pre-commitment superposition) plus a two-dimensional record sector (post-commitment outcomes), with two states insufficient (they would conflate amplitude and record) and six or more non-minimal (they would admit multiple irreducible outcomes). The three routes converge on the same conclusion: $\mathscr{H}_$fold $\cong \mathbb{C}^4$ is overdetermined.

In the language of §4.1, the four basis states are precisely the four states of a fold:

$$(\sigma_i, \omega_i) \in \{(+1, +1), (+1, -1), (-1, +1), (-1, -1)\} \leftrightarrow \{|0, +\rangle, |0, -\rangle, |1, +\rangle, |1, -\rangle\}.$$

The cell-level closure operators U_{ij} act on the discrete (σ, ω) labels of adjacent folds; their continuum image acts on $\mathbb{C}^4$ at each fold. The transport action $S_$int of §4.4 is the cell-level dynamics whose long-time limit, on the attractor subspace, is the unitary evolution on the per-fold $\mathbb{C}^4$ underlying the subsequent gauge analysis.

This correspondence matters because it lets the gauge structure of §6 and the Maxwell transport of §7 be developed on either side of the bridge. The U(1) emergence treated in this paper is what

the cell-level picture sees in the continuum limit; the SU(2) and SU(3) structures developed in the companion programme are what the $\mathbb{C}^4$-level picture sees once additional internal structure is taken into account (see §7's scope note and §8).

---

5. Commitment Dynamics and the Record Field

With the variables of §4 in place, the dynamics of fold formation can be stated precisely. A **fold** is the irreversible terminus of reversible pre-commitment evolution — a committed distinction stabilised against local reversal. The key topological condition is:

Proposition 5.1 (Topological Trapping Condition). *Fold formation is possible at a region of the interface if and only if its local closure pathways become non-recombinable; equivalently, if and only if*

$\beta_1 \geq 1$

for the local closure complex.

The argument runs in two steps. If $\beta_1 = 0$, every closed pathway is contractible, and any apparent commitment can be reversed by following the contracting homotopy — the proposed "fact" admits an undoing, and is therefore not a fact. If $\beta_1 \geq 1$, there exists at least one non-contractible loop; this loop cannot be undone without crossing the closure complex elsewhere, and the fold it carries is therefore stable against local reversal. Stability against local reversal is precisely what it means for a fold to be a fact (Hatcher, 2002, for the algebraic topology background).

In the variables of §4, the β_1 transition corresponds to a configuration in which $\mathcal{C}\_\ell$ exceeds $\mathcal{C}^*$ on at least one closure loop — the threshold $\Theta(\mathcal{C}\_\ell - \mathcal{C}^*)$ fires, the loop's closure operator U_ℓ is fixed, a fold forms, and the local closure complex acquires a non-contractible cycle. The two pictures — topological ($\beta_1 \geq 1$) and dynamical (Θ-firing in S_int) — describe the same physical event from different angles.

Once a fold is formed, it contributes to the **committed record field**

$\rho(x, t)$

defined as the local density of folds. Concretely, introducing a per-loop indicator

$\chi\_\ell(t) = \{\ 0,\ \mathcal{C}\_\ell(t) < \mathcal{C}^*;\ 1,\ \mathcal{C}\_\ell(t) \geq \mathcal{C}^*\ \},$

the record field is

$\rho(x, t) = \Sigma\_\ell\ \chi\_\ell(t)\ \delta^{(3)}(x - x\_\ell),$

i.e. a sum over loops of indicator-weighted delta functions located at the loop sites x_ℓ. The record field is monotonic:

$$\partial_t \rho(x, t) \geq 0,$$

provided $\partial_t \chi_\ell \geq 0$ for every ℓ — committed folds do not uncommit. This conditional monotonicity is structural: an uncommit event would correspond to χ_ℓ stepping from 1 back to 0, which is excluded by the irreversibility of the $\Theta(\mathcal{C}_\ell - \mathcal{C}^*)$ firing in S_{int} (a closure penalty above threshold fixes the loop's closure operator; below-threshold fluctuations no longer return the loop to its pre-commitment state).

The monotonicity also encodes the **Landauer-style** asymmetry between reversible pre-commitment evolution and irreversible fold formation (Landauer, 1961; Bennett, 1982): an irreversible commitment requires a physical recipient for the discarded alternative, and the record field is the operational manifestation of that recipient at the bulk level. This monotonicity is itself the origin of **operational time** in VERSF: the irreversible ordering of record growth provides the substrate on which an arrow of time can be defined, rather than being imposed on it. Time is therefore not a parameter of the Void; it is a derivative property of accumulated interface activity. The framework's underlying informational ontology — physical structure as accumulated, distinguishable, irreversible information — places it in the tradition initiated by Wheeler (1990).

The record field is also the bridge between the interface and the bulk. The interface *generates* $\rho(x,t)$ through fold formation; the bulk *carries* its coarse-grained reconstruction. The two sides of this bridge govern, respectively, the gauge structure of §6 and the geometric structure of §9.

The detailed dynamics of the record field — the wave equation governing the propagation of committed information, the memory kernel encoding accumulated history, and the operative record for geometric sourcing — are developed in companion programme work on the coherence scale and memory kernel reduction. Two consequences of that development matter at the level of the present paper. First, the commitment-capacity threshold (CCC) fixes a unique coherence scale $\xi = (\hbar c/\varepsilon)^{1/4}$ with no free parameters, where ε denotes the local matter/radiation energy density of the region (throughout this paper, ρ is reserved for fold density; ε is used here and below for energy density, to avoid ambiguity): below ξ, fluctuations remain reversible and no folds form; above ξ, folds become possible. The same scale fixes the mass parameter $m = C_m \xi^{-1}$ of the κ-field — the VERSF field sourced by committed events, $(\Box + m^2)\kappa = \rho_{\text{committed}}$ — whose retarded Green function under causal-coherence projection generates a derived memory kernel $K_{\text{sel}}(\tau) = \cos(m\tau)/(2\pi\tau)$ with power-law $(1/\tau)$ persistence and oscillatory structure. Second, as a forward reference to §10: the operative record for geometric sourcing is not the instantaneous fold density ρ alone but the effective record field

$$s_{\text{eff}}(x, t) = \rho(x, t) + \beta_\Xi \, \Xi(x, t)$$

where $\Xi(x, t)$ is the causal memory field accumulating past commitments through the derived kernel and β_Ξ is an O(1) coupling. The instantaneous density ρ of §5 is one term in s_{eff}; the memory term Ξ encodes the full causal-past contribution. Geometry — developed in §§9–10 —

responds to s_eff, not to ρ alone. In the limit $\beta_\Xi \to 0$, or for slowly varying density where memory reduces to a renormalised local contribution, the standard instantaneous picture is recovered.

---

6. Gauge Structure from Interface Encoding Redundancy

The central claim of this section is:

Gauge redundancy is interface encoding degeneracy.

Formalising this:

Lemma 6.1 (Closure-Equivalent Encoding Degeneracy). *Let two interface configurations $\{\varphi_i\}$ and $\{\varphi_i'\}$ generate identical closure operators U_γ for every admissible loop γ on the interface. Then the two configurations are operationally indistinguishable with respect to committed transport observables and belong to the same physical transport equivalence class. Consequently, local re-encodings preserving all loop holonomies act as gauge redundancies of the continuum transport description.*

Proof. Let $\mathcal{X} = \{(\varphi_i, U_{ij})\}$ denote the space of microscopic interface configurations (cell-level fold states together with link variables). Define the **observable map**

$\mathcal{O} : \mathcal{X} \to \{U_\gamma, J_\gamma\}$, $\mathcal{O}(X) = (U_\gamma(X), J_\gamma(X))_\gamma$ admissible,

assigning to each configuration its closure operator $U_\gamma = \prod_{\langle ij\rangle \in \gamma} U_{ij}$ on every admissible loop γ together with the corresponding committed transport currents J_γ. Define the equivalence relation

$X \sim X' \Leftrightarrow \mathcal{O}(X) = \mathcal{O}(X')$.

Two configurations are equivalent precisely when their closure operators and committed transport currents agree on every admissible loop. By construction, the operationally accessible content of a configuration is captured by $\mathcal{O}$: every committed transport observable is a function of $\{U_\gamma, J_\gamma\}$. Therefore configurations in the same equivalence class generate identical physical transport observables, and are operationally indistinguishable. Gauge transformations are precisely the automorphisms of $\mathcal{X}$ that preserve $\mathcal{O}$ — that is, elements of the stabiliser subgroup $\{g : \mathcal{O}(g \cdot X) = \mathcal{O}(X) \text{ for all } X\}$. This stabiliser acts as the gauge group of the continuum transport theory. ■

This is the interface-level origin of gauge redundancy in the VERSF framework. Gauge freedom is therefore not imposed as a mathematical convenience, but emerges from the degeneracy of local interface encodings under identical closure transport.

Concretely, two encodings differing only by a local change of σ-frame or by a globally consistent shift of ω-phase produce indistinguishable physical effects on the committed record. These are the elementary gauge transformations of the substrate. The space of $\{\varphi_i\}$-configurations, modulo the equivalence relation of Lemma 6.1, is the space of *physical* interface states.

The familiar gauge potential

$A\_\mu(x)$

is therefore not a directly observable object in VERSF, and was never expected to be. It is the *coordinate description* of the local interface encoding in continuum form — the smoothed image of the cell-level (σ_i, ω_i) data in a particular frame. Different local choices of frame describe the same physical closure transport.

This structural fact reorganises three standard objects of gauge theory.

Wilson loops. A Wilson loop

$W[\gamma] = \exp(i \oint\_\gamma A\_\mu \, dx\^\mu)$

is, in the interface picture, the continuum image of the closure operator U_γ along a loop γ on the interface (Wilson, 1974). It is gauge invariant — invariant under the equivalence of Lemma 6.1 — because closure phase along a closed loop is a property of the loop itself, independent of which encoding is used to describe it.

Holonomy. Holonomy is the accumulated closure phase around any topologically nontrivial circuit — directly, the eigenvalue of U_γ for non-contractible γ. In VERSF, holonomy becomes a direct *operational* observable: it is the difference in committed phase recorded by an interface region after traversing a closed pathway through the encoding space.

Field strength. The electromagnetic field strength

$F\_\mu\nu = \partial\_\mu A\_\nu - \partial\_\nu A\_\mu$

is the **local failure of closure triviality** — the continuum image of $U\_\{\delta\gamma\} - \mathbb{1}$ for infinitesimal loops δγ. Where $F\_\mu\nu = 0$, every infinitesimal loop closes trivially and the interface admits a globally flat encoding; where $F\_\mu\nu \neq 0$, the interface carries irreducible local curvature in its closure structure.

The standard structural facts of gauge theory — gauge redundancy, Wilson-loop gauge invariance, the geometric meaning of $F\_\mu\nu$ — therefore have a single underlying source in VERSF: they are all consequences of *interface encoding degeneracy modulo identical closure transport*, expressed in the continuum.

---

7. Conserved Closure Transport and the Emergence of Maxwell Structure

Bit Conservation and Balance (BCB), established in earlier programme papers, requires that distinguishability cannot be created or destroyed locally; it can only be redistributed. Applied to the interface, this gives:

Proposition 7.1 (Local Closure Conservation). *Closure transport on the interface obeys*

$$\partial_\mu J^\mu = 0$$

where J^μ is the conserved interface transport current.

The argument is direct from the action of §4. The transport term $\mathscr{A}(\varphi_i, \varphi_j)$ is symmetric under exchange of cells and preserves the sum of orientation and parity quanta on any closed region. Any local non-conservation of J^μ would require local creation or destruction of distinguishability, contradicting BCB. Conservation is therefore not a separate postulate but a direct consequence of the framework's bit-accounting axiom together with the cell-level dynamics of S_{int}.

The continuum behaviour of this conserved closure transport can be stated as a formal limit:

Lemma 7.2 (Continuum Closure Transport Limit). *Let the interface support locally conserved closure transport satisfying:*

- *nearest-neighbour reversible update structure,*
- *loop consistency,*
- *closure-current conservation,*
- *and coarse-grainability over scales $L \gg \xi$ (where ξ is the characteristic interface cell scale).*

Then the leading-order continuum transport equations of the interface take Maxwell form (Maxwell, 1865):

$$\partial_\mu F^{\mu\nu} = \mu_0 J^\nu,$$

together with

$$\partial_{[\lambda} F_{\mu\nu]} = 0,$$

where $F_{\mu\nu}$ is the continuum closure-curvature tensor associated with infinitesimal loop transport. The resulting continuum theory is therefore U(1)-type Abelian gauge transport.

The discrete-to-continuum calculation runs as follows. Site phases θ_i on the cells of the interface define link variables

$U_{ij} = \exp(iaA_{ij})$,

where a is the lattice spacing of the cell complex and A_{ij} is the link-averaged continuum gauge potential. Plaquette holonomies are the loop holonomies of Definition 4.1 around the smallest non-trivial loops:

$U\_p = \prod\_\{\ell \in \partial p\}\ U\_\ell = \exp(ia^2\ F\_\mu\nu + \mathcal{O}(a^3))$,

where $F\_\mu\nu = \partial\_\mu\ A\_\nu - \partial\_\nu\ A\_\mu$ is the continuum field strength and the higher-order terms vanish in the lattice-continuum limit $a \to 0$. The Wilson form of the closure-penalty term in the toy action of §4.4,

$S\_W = \beta\ \Sigma\_p\ (1 - \mathrm{Re}\ U\_p)$,

expands at small a to

$S\_W \approx (\beta\ a^4 / 4) \int F\_\mu\nu\ F\hat{}\mu\nu\ d^4x$,

which is the standard Maxwell action up to normalisation absorbed into μ_0. Variation of S_W with respect to A_μ together with the conserved current $J\hat{}\nu$ of Proposition 7.1 yields the inhomogeneous Maxwell equation $\partial\mu\ F\hat{}\mu\nu = \mu_0\ J\hat{}\nu$. *Loop consistency on the interface — the* $U\{\delta\gamma\} = \mathbb{1}$ condition of §4.3, applied to the boundary of a 3-cell — gives the homogeneous Bianchi identity $\partial[\lambda\ F\_\mu\nu] = 0$ *directly from the discrete substrate; in the continuum this is the geometric statement that* $F = dA$ *is a closed 2-form, since* $d^2 = 0$. *The full admissibility derivation, including non-trivial coefficient determination and the link to hexagonal interface dynamics, is carried out in companion programme work on hexagonal interface light propagation. What the present paper supplies is the substrate layer: the four hypotheses of Lemma 7.2 are precisely those guaranteed by the cell-level dynamics of §4 — the reversible update structure is given by* U_{ij}; *loop consistency is the* $U\{\delta\gamma\} = \mathbb{1}$ condition of §4.3; closure-current conservation is Proposition 7.1; and coarse-grainability follows from the locality of the $\mathscr{L}$-term and the homotopy-only dependence enforced by the closure penalties $\mathcal{C}\_\ell$.

The familiar physical interpretations follow at once:

- **Electric divergence** corresponds to a local imbalance in closure transport — a region of the interface acting as a net source or sink of conserved closure current.
- **Magnetic circulation** corresponds to circulation structure in closure transport — a stable rotational pattern of (σ, ω) updates around a loop.
- **Light** is a propagating oscillatory transport mode of the interface, in which divergence and circulation feed each other through the coupled Maxwell structure.

In this picture, the speed of light is not a primitive constant of the framework. It is the ratio of two interface response rates: the rate at which an orientation perturbation propagates along the σ-structure, and the rate at which a closure-parity perturbation propagates along the ω-structure. These rates are set by the underlying admissibility structure — including the K = 7 constraint dimensionality treated in §8.

A note on scope: Abelian transport and the non-Abelian companion derivations

The closure structure developed here is **Abelian**. The (σ, ω) data on each cell is binary, the cell-level updates U_{ij} act on a two-component state, and the closure operators U_γ commute in their continuum limit. The continuum transport that emerges is therefore U(1)-type — the resulting A_μ field carries a single phase degree of freedom, the resulting $F\_\mu\nu$ has the structure of an antisymmetric two-tensor, and the resulting transport is Maxwell.

The non-Abelian extension is not treated in the present paper. It is, however, developed in two companion programme papers along independent routes.

The companion VERSF synthesis paper deriving spacetime, quantum correlations, and the Standard Model gauge group identifies the full SU(3) × SU(2) × U(1) structure from the three-channel decomposition of the commitment interface by the fundamental theorem of surface theory: the metric (first fundamental form) contributes a scalar channel $\mathbb{C}^1 \to$ U(1); the surface-normal direction of the shape operator contributes a spinorial channel $\mathbb{C}^2 \to$ SU(2); and the three independent components of the shape operator contribute a curvature channel $\mathbb{C}^3 \to$ SU(3) (Yang & Mills, 1954, for the original non-Abelian construction).

Independent companion programme work on the one-fold structure derives the same gauge group along a different route, as the commutant of a $3 \oplus 1$ block-diagonal hopping matrix K on $\mathbb{C}^4$, with the $3 \oplus 1$ decomposition itself derived from the unique gauge-invariant void state combined with $\dim(\mathscr{H}\_\text{fold}) = 4$.

The U(1) sector developed here is therefore **one channel of a fuller picture**. The SU(2) and SU(3) sectors live in the same architecture but require richer interface data than the (σ, ω) treated in this paper.

---

8. The Constraint Dimensionality K = 7

The minimal interface architecture has so far been described qualitatively: cells $\varphi_i = (\sigma_i, \omega_i)$ on an S^2 interface hosting one fold each, governed by the transport action S_int of §4. Companion programme work on the K = 7 constraint dimensionality sharpens this picture in two related respects.

Hexagonal tiling. The commitment interface must be tiled by regions of equal area; the perimeter-minimising tiling is uniquely hexagonal by the Honeycomb Theorem (Hales, 2001). The choice is forced rather than free, and the perimeter–area argument is only one of several convergent reasons: companion programme work on hexagonal interface light propagation shows that hexagonal coordination is uniquely selected by four independent arguments — perimeter-minimisation (the Honeycomb Theorem), dispersion-symmetry analysis (six-fold pushes the leading anisotropic angular harmonic to $\cos(6\theta)$ at order $|k|^6$, whereas four-fold permits $\cos(4\theta)$ at order $|k|^4$), renormalisation-group flow (hexagonal anisotropy decays as b^{-4} under coarse-graining, two orders faster than square), and information-theoretic optimality (the

60° angular gaps of six-fold coordination annihilate all low-order angular harmonics m = 1, 2, 3, 4, 5). The convergence of these four independent channels on the same lattice is what underwrites the K = 7 appeal to hexagonal structure. This is the lattice that supports the cells φ_i of §4 — each hexagonal cell hosting one fold.

Constraint dimensionality. The integer **K** counts the independent binary admissibility constraints that any region of the interface must satisfy to support stable fold formation. The number of distinguishable admissible configurations on a Planck-area patch is 2^K. The K = 7 companion work establishes the value by six labelled arguments — reducing under independence analysis to four genuinely distinct mathematical frameworks: geometric closure, binary gauge encoding, topological integrality on the de Sitter horizon, and combinatorial balance.

K = 7 is the unique positive integer at which all four frameworks are simultaneously satisfied.

A sketch of how each framework contributes:

- **Geometric closure.** A rank-nullity analysis on the hexagonal interface constraint network gives K = 6 + 1 = 7 — six independent boundary directions per hexagonal cell plus one global closure mode tying the surface together.
- **Binary gauge encoding.** The interface must encode the pairwise relations among the Standard Model's twelve generators. There are C(12, 2) = 66 such relations, requiring $2^K \geq 66$, giving $K \geq \lceil \log_2 66 \rceil = 7$ from below; an overdetermination argument gives the matching bound from above.
- **Topological integrality.** Chern–Weil integrality of the U(1) winding number on the de Sitter cosmological horizon requires $n(K) \in \mathbb{Z}^+$. The winding number is super-exponentially sensitive to K, with adjacent integer values shifting n by ~53 orders of magnitude. Only K = 7 lands in the cosmologically observed window.
- **Combinatorial balance.** The integer-exact Diophantine equation $2^K + 8 = N(N - 1)/2$ has the unique positive-integer solution K = 7, N = 17 (where N is the channel count entering the binary gauge encoding bound). This is the strongest single result of the K = 7 paper: fully unconditional, shared with no other constraint, and verified by exhaustive integer search.

The hexagonal cell structure also supports a definite **loop count**. Two adjacent hexagonal cells share one edge, giving 6 + 6 − 1 = 11 boundary edges. Each of the two interior vertices of the shared edge supports an additional non-edge loop — a path traversing the boundary and returning through the cell interior — contributing 2 further independent closure loops. A final global closure mode ties the surface together, giving

$N\_\text{loop} = 11 + 2 + 1 = 14.$

This is the channel count that appears in the bare electromagnetic coupling derived in the companion programme.

For the present paper, the implications are structural rather than numerical.

First, the **hexagonal structure** of the interface is forced, not chosen. The cells φ_i of §4 are hexagonal, and the closure operators U_γ of §4.2 act on closure loops with the structure described above.

Second, the **constraint dimensionality K = 7** is what permits the binary gauge encoding of the twelve Standard Model generators on the interface. The U(1)-type Maxwell emergence of §6 and §7 is one channel of this broader encoding.

Third, the **fine-structure constant** acquires a derivation from interface geometry in companion work. Two routes appear in the programme — the internal-geometry route (one-fold structure) gives $\alpha = (1/12)^2 \approx 1/144$ from democratic curvature allocation across the twelve generators on $\mathbb{CP}^3$, with a $3 \oplus 1$ impedance correction yielding $\approx 1/137$; the constraint-dimensionality route (K = 7 architecture) gives a bare coupling $\alpha^{-1}_{bare} = 2^7 \cdot 15/14 \approx 137.143$, with a residual ≈ 0.1 gap to the observed 137.036 attributed to a second-order inverse-participation-ratio correction. Both routes have residual gaps under active analysis, and the apparent numerical coincidence between them is itself a structural target of the reconciliation programme — not yet a confirmation that either route is complete.

The K = 7 architecture is therefore **not a property of the interface taken in isolation**. It is the constraint dimensionality of admissibility itself — the minimum number of independent ways any region of physical reality must agree with itself in order to stably exist. The commitment interface is the substrate on which this dimensionality is realised; K = 7 is the integer that the substrate is required to satisfy.

---

9. Geometry as Record Reconstruction

The geometric reconstruction developed in this section operates at the **coarse-grained bulk level** — large-scale correlations of the accumulated record $\rho(x, t)$. Before turning to it, one preliminary question deserves note: how does a 3D bulk arise from a 2D interface in the first place?

9.1 From 2D Interface to Bulk Reconstruction

The working answer is developed across a three-paper cluster in the programme. Companion programme work on hexagonal interface light propagation gives the calculational picture: bulk distance defined operationally via correlation decay between interface points across a coarse-graining scale index z. Further companion programme work argues that depth itself fails the structural criteria (intrinsic metric, locality, propagation, reversibility) that define spatial directions, and is properly a descriptive index rather than a kinematic axis. A third strand supplies the explicit positive construction: depth $z(s, s')$ is defined as the minimum number of updates after which two configurations on the 2D interface become operationally indistinguishable — $z(s, s') = \min\{N : s \sim_n s'\}$ — the physical depth coordinate is $Z = \kappa z$ (with units of length), and a reconstruction functional $\mathscr{F}$ produces an effective (2+1+1)-dimensional spacetime metric $ds^2 = -c^2 d\tau^2 + g_{ab}(x) dx^a dx^b + dZ^2$ in which the third spatial coordinate is

the persistence-axis of distinguishability across the sequence of interface updates. Emergent space therefore arises from the temporal sequencing of fold commitments on the interface, with the third dimension a derived coordinate, not an independent kinematic direction.

At a finer level, the record itself organises into a discrete causal partial order $(\mathcal{C}, \leq, \varphi)$, where $\mathcal{C}$ is the set of folds (committed distinctions) ordered by causal precedence. The causal partial-order treatment, developed in the VERSF synthesis paper on spacetime, quantum correlations, and the Standard Model gauge group, recovers Lorentz covariance from the non-foliability of $(\mathcal{C}, \leq)$: no global simultaneity surface can be cut, so no preferred frame is selectable by any observer. The treatment relates closely to causal-set theory (Bombelli, Lee, Meyer & Sorkin, 1987), with fold admissibility playing the structural role that Poisson sprinkling plays in the original causal-set programme. The remainder of this section addresses the further question: given that the bulk emerges from the temporal sequencing of fold commitments on the interface as outlined above, what is the effective continuum geometry that the accumulated record loads onto that emergent bulk?

9.2 Coarse-Grained Geometry from the Accumulated Record

The committed record field $\rho(x,t)$ is the accumulated density of folds. By §5, it grows monotonically wherever interface activity is occurring. The geometric content of VERSF appears when we ask what large-scale structures emerge from this accumulation.

Define the effective entropy field

$s(x) = \log \rho(x, t)$

(up to additive normalisation), describing the large-scale loading structure of the record. The Void responds to gradients of $s(x)$ by modulating the rates at which subsequent folds can form in nearby regions: high-loading regions transport less efficiently, low-loading regions transport more efficiently. This is not an imposed dynamical law — it is a direct consequence of finite distinguishability capacity in the Void's constraint structure.

The proper development of the effective metric requires moving beyond scalar dynamics, since scalar closure of record accumulation cannot encode the directional and relational structure that gravitational phenomena exhibit — the scalar trace assigns a magnitude at each point but no preferred axis, so anisotropic tidal structure and curvature (which is intrinsically pairwise) cannot be sourced by a scalar alone. As established in companion programme work on gravity from tensorial closure of record dynamics, the scalar record density ρ of §5 is properly understood as the trace Φ = g^{μν} Φ_{μν} of a more fundamental symmetric rank-2 commitment-density field Φ_{μν}, and the emergent metric is g_{μν} = Φ_{μν}/λ_★ — derived rigorously from closure-consistent parallel transport plus pointwise commitment commutativity, not from a scalar-derivative ansatz. The structural claim of this section — that geometry is the bulk reconstruction of interface-generated record structure — remains correct; what changes is the recognition that the operative record field is tensorial, with the scalar of §5 its trace projection. The detailed gravitational dynamics are taken up in §10.

Geometry is therefore, in VERSF:

the large-scale reconstruction of interface-generated record structure.

Spacetime in this picture is not a stage on which physics occurs. It is the integrated history of the interface's activity, expressed in coarse-grained form. The proposal that geometry is reconstructed rather than fundamental places the framework in dialogue with the holographic principle ('t Hooft, 1993; Susskind, 1995), though the reconstruction here proceeds from interface fold-formation dynamics rather than from a boundary–bulk duality.

---

10. Gravity as the Tensorial Closure of Record Dynamics

The schematic picture of §9 — that the effective metric reconstructs interface-generated record loading — is developed rigorously in companion programme work on gravity from tensorial closure of record dynamics. The present section surfaces that work's main results and locates them in the architecture developed here.

The high-level physical narrative is unchanged from the schematic version:

- **High record density** suppresses local fold formation (the Void's distinguishability capacity is partially saturated);
- this **reduces local tick efficiency** (folds form less frequently per Void-cycle);
- which in turn **modifies effective causal structure** in the way that an observer at the scale of the coarse-grained metric will describe as curvature.

The following short consolidating statement separates three distinct objects that the reader should keep distinct throughout this section:

Theorem 10.0 (Rank-2 minimality and tensor separation). If the record source couples universally to all committed energy-momentum configurations and the response is local, symmetric, and covariant, then the minimal admissible response object is rank-2. The fundamental gravitational object is therefore a symmetric rank-2 commitment-density field

$\Phi_{\mu\nu}$,

the emergent metric is

$g_{\mu\nu} = (1/\lambda_{\bigstar})\, \Phi_{\mu\nu}$,

and the Einstein dynamics take the form

$G_{\mu\nu} + \Lambda\, g_{\mu\nu} = \kappa\, T^{(\Phi)}_{\mu\nu}$.

The closure current $\mathcal{C}^{\mu\nu}$ (linear in Φ, leading-order record transport), the metric $g_{\mu\nu}$ (geometric structure of the emergent manifold), and the stress-energy tensor $T^{(\Phi)}_{\mu\nu}$ (quadratic in Φ, source of Einstein curvature) are three distinct objects, none of which should be conflated with the others.

The four structural results below unpack Theorem 10.0:

1. **Rank-2 selection (Theorem 1 of the companion programme work).** Among all finite-dimensional irreducible representations of SO(3,1) admitting a universal local coupling to the committed energy-momentum source, the unique minimal admissible response sector is the symmetric rank-2 representation $(1,1) \oplus (0,0)$ — by a Schur-type lemma applied to the intertwiner constraint at bilinear, zero-derivative order. Scalar closure is structurally insufficient (it couples only to the trace of the source); vector and antisymmetric rank-2 candidates are ruled out at leading order by representation-theoretic impossibility. The fundamental gravitational object is therefore a symmetric rank-2 commitment-density field $\Phi_{\mu\nu}$, whose metric trace $\Phi \equiv g^{\mu\nu}\,\Phi_{\mu\nu}$ recovers the scalar record density ρ of §5 as a trace projection of the tensorial sector.
2. **Linear leading-order uniqueness (Theorem 2).** Within the linear, local, zero-derivative-in-Φ ansatz, the leading-order record current is uniquely $\mathcal{C}^{\mu\nu} = a\,\Phi^{\mu\nu} + b\,g^{\mu\nu}\,\Phi$ — the closure analogue of the trace-reversed metric perturbation of linearised general relativity. Crucially, $\mathcal{C}^{\mu\nu}$ (linear in Φ, dim M^1) is *distinct from* the stress-energy tensor $T^{(\Phi)}_{\mu\nu}$ (quadratic in Φ, dim M^4) that sources Einstein curvature.
3. **Metric emergence (Theorem 3).** Closure-consistent parallel transport of committed structure, combined with the pointwise commutativity of the substrate commitment algebra (listed in the companion programme work as supplementary corpus input (E5)), determines a unique torsion-free connection. Non-degeneracy of $\Phi_{\mu\nu}$ — forced by universality of the source — identifies $\Phi_{\mu\nu}$ as a metric, and the fundamental theorem of Riemannian geometry identifies the connection as the Levi-Civita connection of $g_{\mu\nu} = \Phi_{\mu\nu}/\lambda_{\bigstar}$, where $\lambda_{\bigstar}$ is the local commitment-density scale fixed by finite distinguishability. The metric is therefore not a postulate but the unique structure compatible with closure-consistent transport of committed records.
4. **Einstein dynamics.** Lovelock's theorem applied to the emergent geometric sector selects the Einstein form $G_{\mu\nu} + \Lambda\,g_{\mu\nu} = \kappa\,T^{(\Phi)}$*{μν} as the unique low-derivative covariant closure, sourced by T^{(Φ)}*{μν} rather than by $\mathcal{C}^{\mu\nu}$. The standard Lovelock hypotheses — covariance, second-order, divergence-free, symmetric rank-2 — are themselves derivable from the programme's closure constraints.
5. **Non-Markovian temporal extension.** The four results above cover the instantaneous case. Companion programme work on the coherence scale and memory kernel reduction extends the construction to history-dependent sourcing, replacing the instantaneous fold density ρ by the effective record field $s_{eff} = \rho + \beta_{\Xi}\,\Xi$ (where Ξ accumulates past commitments through the derived κ-field memory kernel $\cos(m\tau)/(2\pi\tau)$ with $m = C_m\,\xi^{-1}$), and producing linearised metric perturbations with oscillatory power-law memory $\delta g_{\mu\nu} \propto \beta_{\Xi}\cos(mt)/t$. In the Markovian limit (slow commitment density), results (3)–(4) are recovered intact.
6. **Scalar Newtonian limit and a second route to linearised GR.** Companion programme work on gravity from fold density gradients develops the scalar Newtonian limit

independently — deriving the Poisson equation $\nabla^2\Phi_{bound} = 4\pi\lambda c^2\xi\,\rho_{bound}$ from continuity, the unique linear isotropic constitutive law, and the unique scalar source identification (bound committed distinguishability) — and reaches the same linearised Einstein structure through a second route, the 6+1 hexagonal closure architecture of the fold interface producing the Fierz–Pauli coefficient pattern (1, −2, −1, +2) through four structural steps. A binary suppression law $\lambda/\mathcal{C} = 2^{(-2KN_{loop})} \cdot (1/N_{loop})$ with K = 7 and N_{loop} = 14 explains the ~60-orders-of-magnitude weakness of gravity as a theorem of fold architecture rather than as fine-tuning; the coherence scale $\xi_{coh} \approx 79$ μm forced by the suppression law reproduces the observed G to ~2%, with a structurally-derived bridge exponent $\gamma = 3/8$ connecting it to the QCD-scale anchor $\xi_{fold} \approx 0.6$ fm. Full derivational status, the explicit C[h] closure-functional construction, and the fold-sector transport algebra completing the $\gamma = 3/8$ proof are deferred to that companion work.

7. **Capacity-saturation reframing.** Companion programme work on gravity as critical entropic back-pressure operates at the macroscopic-response layer (see the sixth scope note in §11.3): it reframes gravity as void back-pressure — the void resists additional distinguishability, suppressing the efficiency with which ticks stabilise into bits, with proper-time gradients bending worldlines inward — derives the Schwarzschild radius $r_s = 2GM/c^2$ from a global areal-saturation condition ($\int_S \Sigma\, dA = \Sigma_c \cdot A$) rather than from divergent curvature, and proposes that the same finite-capacity principle governing gravity also governs the quantum–classical transition through different interfaces (global/areal for gravity, local/redundant via projection efficiency $\alpha_{env} \ll 1$ for environmental decoherence). The unified picture is offered as a conceptual reframing of the quantum-gravity problem, not as a replacement for microscopic quantum gravity programmes.

Gravity in VERSF is therefore not fundamental curvature imposed on a fundamental spacetime. It is the **Void's response to interface-generated record loading**, expressed rigorously as the unique tensorial closure of record dynamics consistent with universal coupling to the committed energy-momentum source. The construction is post-emergence: it derives the leading-order tensorial dynamics on the already-emerged 4-manifold M, with the existence, dimension, smooth structure, and Lorentzian signature of M carried as explicit corpus inputs (E1, E2) rather than re-derived. A construction running from substrate directly to dynamics in a single paper is reserved for a separate stage of the master-action roadmap.

The companion programme work closes with four sharp empirical falsifiers targeting the rank-2/Lovelock construction:

- **(F1)** Detection of antisymmetric rank-2 phenomenology mimicking gravity in gravitational-wave polarisation modes — testable via the LIGO–Virgo–KAGRA general-polarisation framework, sharpened by the five-detector Eardley threshold met by next-generation observatories. Detection would falsify the source-identification step in additivity (C4), not Theorem 1 itself.
- **(F2)** Frequency-dependent gravitational-wave dispersion at order $(\omega/M_{\bigstar})^2$, testable in BNS-class events of GW170817 type with multimessenger electromagnetic counterparts, with sensitivity in $M_{\bigstar}$ tightened by roughly an order of magnitude by Einstein Telescope, Cosmic Explorer, and LISA.

- **(F3)** Inverse-square-law deviations at low density that do *not* follow the predicted parametric form ~ (ρ/ρ_★) — would falsify either Theorem 2 or the suppression-scale argument underlying it.
- **(F4)** Non-vanishing antisymmetric component of the gravitational connection — testable through tests of the equivalence principle for spinning bodies; detection would falsify the (E5) pointwise commitment commutativity input and force a non-abelian substrate commitment-algebra at the resolution scale ℓ_★.

Empirical signatures of results (5)–(7), together with the cavity-physics 6Ω signature and the quantum-simulator 2:1 MERA correlation-asymmetry signature surfaced earlier in the programme, are summarised in §11.3 with citations to their respective companion papers. The tight conceptual link between gravity, geometry, entropy, and information — long noted in the gravitational thermodynamics literature, beginning with Bekenstein (1973) and Hawking (1975), and developed in the equation-of-state derivations of Jacobson (1995) and the entropic-force programme of Verlinde (2011) — appears here as a structural consequence of the framework's architecture rather than as a coincidence demanding explanation. Within the VERSF programme, this account of gravity at the coarse-grained bulk level complements the causal-set treatment of the companion synthesis paper, which derives Lorentz covariance at the finer level of the discrete partial order of folds.

---

11. Interpretive Context

The three subsections that follow situate the paper's claims relative to standard gauge theory, exhibit their internal dependency structure, and fix their scope and conditionality.

11.1 Comparison with the Standard Picture

The contrast between standard gauge theory and the VERSF interface picture can be summarised compactly.

Standard picture	VERSF picture
Gauge symmetry is fundamental	Gauge redundancy emerges from interface encoding degeneracy
Fields live in spacetime	Transport lives on the commitment interface; spacetime is reconstructed
Geometry is fundamental	Geometry is the coarse-grained reconstruction of the record
Maxwell equations are postulated	Maxwell transport is the hydrodynamic limit of closure transport
Time is an external parameter	Time is the ordering of irreversible record growth
Continuum from the outset	Continuum from coarse-graining of discrete interface cells

Each row records a structural relocation. What standard gauge theory takes as primitive, VERSF takes as derived from the closure dynamics of a more fundamental substrate. The two pictures are not in conflict at the level of empirical predictions in the regimes covered by Maxwell theory; they differ in what they identify as the ontological floor.

This is not the claim that standard gauge theory is mistaken. It is the claim that standard gauge theory is *complete at its own level of description* while leaving open the question of what supports that description. The VERSF interface picture proposes an answer to that question — a substrate at which gauge structure, Maxwell transport, and geometric reconstruction acquire common closure-theoretic origins.

11.2 Dependency Structure of the Interface Programme

The logical and derivational dependencies between the structures developed in this paper form a single vertical chain:

```
Void looplessness (β₁ = 0)
        ↓
Commitment interface (closure-bearing 2-surface)
        ↓
Stable closure pathways (loops)
        ↓
Topological trapping (β₁ ≥ 1)
        ↓
Fold formation (committed distinctions)
        ↓
Record accumulation ρ(x,t)
        ↓
Closure-current conservation
        ↓
Gauge redundancy from encoding degeneracy
        ↓
Maxwell-form continuum transport
        ↓
Bulk geometric reconstruction
        ↓
Gravity as record-loading response
```

Each link is a *derivational* step: the lower structure follows from the upper one given the framework's admissibility constraints, not a parallel layer that must be independently postulated. The ontological chain of Figure 1 displays the same structure with the gauge/geometry fork made visible; the present chain emphasises the linear logical sequence of derivations.

11.3 Scope and Conditionality

Several claims of the present paper should be read with precise scope.

First, the paper does not derive the detailed microscopic substrate dynamics from first principles. The interface transport action introduced in §4 is **structural rather than fully constructive**, and should be understood together with the discrete transport and Wilson-type

substrate constructions developed in companion VERSF transport papers, and with the explicit derivations of $\mathbb{C}^4$ structure across the convergent VERSF programme routes referenced in §4.5.

Second, the emergence of Maxwell-form transport in §7 should be read as the emergence of **admissible U(1)-type continuum transport from closure-preserving interface dynamics**, rather than as a complete standalone derivation independent of the earlier admissibility programme. Lemma 7.2 is a continuum-limit statement that rests on the cell-level structures developed in §4 and on the broader transport derivations of earlier programme papers.

Third, the present paper develops only the **Abelian closure sector**. The non-Abelian sectors SU(2) and SU(3) are derived along independent routes in the companion programme, summarised in §7's scope note and connected to the K = 7 architecture in §8.

Fourth, three points about the gravitational sector of §10. *(i) The treatment is no longer schematic.* Companion programme work on gravity from tensorial closure of record dynamics is the canonical derivation: under the closure constraints (C1)–(C6) plus the supplementary corpus inputs (E1)–(E5) — smooth 4-manifold, Lorentzian signature, EFT power-counting, substrate-level commitment ordering, and pointwise commitment commutativity — Schur's lemma on the universal intertwiner forces rank-2 selection, leading-order linear uniqueness of the record current follows, metric emergence follows from closure-consistent transport, and Lovelock's theorem applied to the emergent geometric sector selects Einstein dynamics. This is the closure of §9 referred to by results (1)–(4) in §10. *(ii) Parallel routes from other directions function as convergence checks rather than independent rederivations.* The 6+1 hexagonal closure architecture of companion programme work on fold density gradients arrives at the same linearised Fierz–Pauli structure from below; a Jacobson-style thermodynamic argument in companion programme work on bit conservation arrives at full nonlinear Einstein equations from one layer above (Layer 1 BCB), with the Bekenstein–Hawking area entropy derived rather than postulated via BCB bit-flux. Convergence across these routes is internal evidence of consistency — the routes share the closure-constraint architecture that underlies the canonical derivation — not three independent derivations of new content. *(iii) The unified gauge–geometry coupling at the level of a single action is the major open structural item, developed in §12.* A candidate VERSF master action S_VERSF governing fold dynamics on the interface, the closure transport of §6–§7, and the tensorial gravitational closure of §10 together — with associated renormalisation-flow structure and anticipated fixed-point hierarchy — is stated in §§12.1–12.5. The first concrete computational instances of the programme — explicit block-fold RG flow with a non-trivial gauge fixed point, first-pass critical-exponent estimates, the conservation-fixed closure-response kernel, the constrained leading-order uniqueness of the local record-current functional $C^{\mu\nu}[\Phi]$, the structural decomposition of $SU(3) \times SU(2) \times U(1)$ from $\mathscr{H}_{\text{fold}} \cong \mathbb{C}^4$, an explicit Monte Carlo recipe, and first preliminary numerical diagnostics — are developed in §§12.6–12.13. Making the full programme rigorous (derivation of the fixed-point structure rather than its conjectural statement, universality-class exponents from substrate dynamics rather than from Ising baselines, completion of the decisive $\lambda^* \neq 0$ lattice test, proof that the non-Abelian decomposition is uniquely selected rather than merely allowed) is the natural next phase of programme work, alongside the relationship to the causal-set treatment of the VERSF synthesis paper — bulk coarse-graining here, partial-order Lorentz emergence there.

Fifth, the present paper does not derive direct experimental signatures of its own, but the wider programme provides empirical handles across five sectors. At the cavity-physics scale, companion programme work on hexagonal interface light propagation predicts a $\cos(6\theta)$ angular harmonic in precision rotating-cavity light-speed measurements, accessible to current $\Delta c/c \sim 10^{-17}$ sensitivities and discriminating the hexagonal interface picture from frameworks designed to preserve exact Lorentz symmetry in the continuum limit (the discriminating power depends on the specific implementation: residual discreteness signatures are an active research topic in the causal-set community, for example). At the quantum-simulator scale, companion programme work on emergent depth predicts a 2:1 $\langle OO\rangle$_boundary/$\langle O'O\rangle$_depth correlation asymmetry in MERA-style architectures. In the gravitational-wave sector (structural / instantaneous), the tensorial-closure work referenced in §10 derives the four falsifiers (F1)–(F4). In the gravitational-wave sector (temporal / non-Markovian) and the coherence-scale sector, the coherence-scale and memory-kernel work predicts slow oscillatory ring-down modulation at frequency $m \sim \xi^{-1}$ (mHz–Hz for stellar-density environments, accessible to LISA), large-angle CMB anomalies if ξ during recombination was macroscopic, and a universal $\varepsilon^{-1/4}$ scaling of decoherence onset (with ε denoting matter/radiation energy density, distinguished from fold density ρ); companion work on fold density gradients adds reduced effective gravitational coupling in coherent quantum systems, together with two internal anchors for the coherence scale (ξ_fold ≈ 0.6 fm and ξ_coh ≈ 79 μm, bridged by $\gamma = 3/8$) reproducing the observed G to ~2%. In the horizon / capacity-saturation sector, companion work on gravity as critical entropic back-pressure adds a smooth $O(\ell_p)$–$O(10^3 \ell_p)$-thick saturation layer in place of a sharp horizon (testable through near-horizon ringdown phenomenology, in principle accessible to LISA), Hawking temperature corrections $\delta T_H/T_H \sim O(\ell_p/r_s)$, gravitational decoherence in height-superpositions driven by differential entropy loading, and a universality check on α_env across decoherence experiments. Detection or null results in any of these channels constitute empirical tests of the programme.

Sixth, the seven gravity results of §10 and the broader machinery of this paper span multiple layers of the BCB–VERSF programme, as articulated in companion programme overview work on the hierarchical structure of the gravity papers. The programme distinguishes five levels of description:

(i) **Physical Admissibility** (Layer 0), the universal admissibility constraints — *Finite Distinguishability* (with finite resources, only finitely many states are reliably distinguishable) and *Irreversible Commitment* (some physical processes are operationally non-invertible) — articulated in companion programme work on physical admissibility as a constraint-based foundation for physics. These are not hypotheses about forces or fields but operational constraints on what any physical theory can do, analogous to unitarity, causality, or the second law — ruling out hypercomputation, unbounded information density, and cost-free erasure while enforcing entropy monotonicity and (given quantum axioms) unitary structure.

(ii) **BCB** (Layer 1), the foundational explanatory principle beneath dynamics: distinguishability obeys a local conservation law; differences cannot be created or destroyed, only flow. From this single principle, companion programme work on bit conservation derives — at this BCB layer rather than at the substrate-structural layer of results (1)–(6) — the Newtonian limit (the static BCB equation reduces to a Poisson equation $\nabla^2 S = 4\pi G\rho_m$ for the entropy potential, with

Fisher information $|\nabla\rho|^2/(4\rho)$ identified as the distinguishability density, and the inverse-square law forced by 3D geometry of conserved flow); the Lorentzian causal structure (the throughput bound $|J_s^i/J_s^0| \leq c$ on bit-current generates a null-cone structure, which determines the conformal class of the metric via the Alexandrov–Zeeman theorem); and Einstein's full nonlinear field equations $G\mu\nu = 8\pi G\, T\mu\nu$ (via a Jacobson-style thermodynamic argument in which the postulated Bekenstein–Hawking area entropy $S = A/(4G)$ is *replaced* by a BCB-derived bit-flux entropy $dS_{BCB} = \int J_s^u\, k\mu\, d\lambda\, dA$, so the area–entropy relation follows from distinguishability flow across the horizon rather than being assumed). The dual appearance of gravity as both geometric curvature and entropy flow is therefore exhibited as a structural consequence of distinguishability conservation rather than a coincidence demanding explanation. The matter–distinguishability coupling $\sigma = 4\pi G\varphi\rho_m$ is motivated by scaling arguments (mass as microstate capacity, energy density as state-transition rate, $T^{00} \leftrightarrow \rho_m c^2$ correspondence) but its numerical coefficient remains phenomenologically fixed by matching to Newtonian gravity, an open item flagged honestly within that work.

(iii) **TPB** (Layer 2), the dynamical layer governing measurement and record formation — tick accumulation toward bit stabilisation, with the Born rule emerging as the equilibrium distribution of iso-entropic branch competition.

(iv) **Critical-capacity VERSF** (Layer 3), the macroscopic response of space to finite distinguishability capacity — capacity strain, suppression of proper-time rates under entropy loading, horizons as global saturation surfaces, and decoherence as local saturation of the same capacity.

(v) The **effective field-theoretic and geometric** description (Layer 4): scalar fields used for phenomenological clock-rate modulation and capacity-strain spatial organisation, together with the geometric language of metric, curvature, and Einstein's field equations themselves — bookkeeping devices encoding how distinguishability flow and capacity constraints appear at large scales, *not* fundamental ontology. This is why General Relativity works so well without being the deepest description.

Within this hierarchy, the present paper develops the **substrate-level structural layer** between Layer 1 and Layer 4: the commitment interface as physically active substrate, the fold architecture ($\mathscr{H}_{fold} \cong \mathbb{C}^4$, the non-emergent 2D character, the K = 7 admissibility count), the closure transport that becomes Maxwell, the record current that becomes geometry, and the tensorial closure of (1)–(4) that becomes Einstein. The temporal extension (5) and the binary-suppression / 6+1 emergence of (6) operate at this same structural layer. The capacity-saturation development of (7) operates at the macroscopic-response layer (Layer 3) above it — interpretive synthesis of how the structural layer manifests in extreme regimes (horizons, decoherence), not a competing technical derivation. None of the structural results invokes effective scalar fields, curvature, or Einstein's equations as fundamental ontology; those appear only as derived collective variables and bookkeeping descriptions of the substrate-level architecture. The hierarchical clarification prevents two specific category errors: treating Layer-4 effective descriptions (scalar fields, curvature, Einstein's equations) as fundamental ontology rather than as bookkeeping; and treating BCB or Physical Admissibility as hidden-variable models or

competing gravity theories rather than as the meta-constraints that any consistent physical theory must encode.

11.4 Mathematical Dependency Table

The following table summarises the formal status of the principal claims developed in the present paper. Three statuses are distinguished: **definition** (a stipulated structural object), **proven** (derived within this paper from its stated premises), **conditional derivation** (derived within this paper subject to a clearly identified hypothesis), and **companion-derived** (proved in a specified companion paper and used here as an external input). Equation labels are shorthand keys to the relevant statement, not new notation.

Claim	Equation / formal content	Status
Interface state space	$\Sigma \cong S^2$ tiled by hexagonal cells; $\mathscr{H}_R = \bigotimes_{i \in R} \mathscr{H}_{\text{fold}}$ (Definition 4.1)	Definition
Fold cell state	$\varphi_i = (\sigma_i, \omega_i) \in \mathbb{Z}_2 \times \mathbb{Z}_2$	Definition
Per-fold Hilbert bridge	$\mathscr{H}_{\text{fold}} \cong \mathbb{C}^4$ (§4.5)	Companion-derived (three convergent routes in VERSF programme work)
Non-emergent 2D character	$D = 2$ maximal under budget admissibility *and* minimal under fact-localisation (§3)	Companion-derived (two convergent routes in VERSF programme work)
Transport action (toy form)	$S_{\text{int}} = J\,\Sigma(1 - \sigma_i\sigma_j) + K\,\Sigma(1 - \omega_i\omega_j) + \lambda\,\Sigma(1 - \text{Re}\,U_\ell) + \Sigma\,\Theta(\mathcal{C}_\ell - \mathcal{C}^*)$ (§4.4)	Definition
Loop holonomy	$U_\ell = \prod_{\langle ij \rangle \in \ell} U_{ij}$	Definition
Topological trapping	Fold formation $\Leftrightarrow \beta_1 \geq 1$ (Proposition 5.1)	Proven
Record density	$\rho(x,t) = \Sigma_\ell\, \chi_\ell(t)\, \delta^{(3)}(x - x_\ell)$ (§5)	Definition
Record monotonicity	$\partial_t\, \rho \geq 0$ (given $\partial_t\, \chi_\ell \geq 0$)	Proven
Coherence scale	$\xi = (\hbar c/\varepsilon)^{1/4}$	Companion-derived (VERSF programme work on coherence scale and memory kernel)
Gauge equivalence	$X \sim X' \Leftrightarrow \mathcal{O}(X) = \mathcal{O}(X')$ (Lemma 6.1)	Proven
Field strength (continuum limit)	$F_{\mu\nu} = \partial_\mu A_\nu - \partial_\nu A_\mu$ from $U_p = \exp(ia^2 F_{\mu\nu} + \mathcal{O}(a^3))$	Conditional derivation (lattice → continuum, $a \to 0$)
Maxwell transport	$\partial_\mu F^{\mu\nu} = \mu_0 J^\nu$ *and* $\partial[\lambda\, F_{\mu\nu}] = 0$ (Lemma 7.2)	Conditional derivation (hypotheses of Lemma 7.2)
K = 7 / N_{loop} = 14 architecture	Diophantine $2^K + 8 = N(N-1)/2$ with unique solution $K = 7$, $N = 17$	Companion-derived (VERSF programme work on the K = 7 constraint dimensionality)

Claim	Equation / formal content	Status
Metric emergence	$g_{\mu\nu} = (1/\lambda_\star)\,\Phi_{\mu\nu}$ (Theorem 10.0)	Companion-derived (VERSF programme work on tensorial closure of record dynamics)
Einstein dynamics	$G_{\mu\nu} + \Lambda\, g_{\mu\nu} = \kappa\, T^{(\Phi)}_{\mu\nu}$	Companion-derived (canonical: tensorial-closure construction; convergence: fold-density-gradients and bit-conservation routes)
Master action	$S_{VERSF} = S_\Sigma + S_M$ (§12.1); first computable RG flow with non-trivial gauge fixed point $g^{*2} = 16\pi^2\,\eta_{fold} / b_0$ (§12.6)	First computable instance; Conjecture 12.1
Closure-response kernel	$K_{\mu\nu}(x, x')$ with $\Phi_{\mu\nu} = \int K_{\mu\nu}(x, x')\,\rho(x')\,d^4x'$ (§12.8); conservation-fixed form $K_{\mu\nu} = \lambda_K [m^2 g_{\mu\nu} G_m + \nabla_\mu \nabla_\nu G_m]$ from $A = Bm^2$ (§12.9)	First computable instance
Local record-current functional	$C^{\mu\nu}[\Phi] = a\,\Phi^{\mu\nu} + b\,g^{\mu\nu}\,\Phi$ from six physical constraints at leading order (§12.10)	First computable instance; Theorem 12.2
Non-Abelian / Yang–Mills extension	$S_{VERSF} \to_{RG} S_{YM} + S_{Einstein} + S_{memory}$ (§12.11); $SU(3) \times SU(2) \times U(1) \subset Aut(\mathscr{H}_{fold})$ from $\mathbb{C}^4 = \mathbb{C}^3 \oplus \mathbb{C}^1$ decomposition	Structural decomposition; uniqueness open

The table is not exhaustive — many supporting propositions and lemmas in the companion programme are omitted — but it identifies the formal load-bearing claims of the present paper and locates each in its appropriate status category. Claims marked *Companion-derived* are not re-proved here; their derivations are imported as external inputs, with the citation indicating where the proof lives.

The central claim of the paper is therefore *structural*:

that the physically active layer of the VERSF substrate is the closure-bearing commitment interface on which folds form, and that gauge transport, record formation, geometry, and gravity all emerge from its closure dynamics.

---

12. Toward a VERSF Master Action and Renormalisation Flow

The preceding sections identify the commitment interface as the physical substrate on which fold formation, closure transport, gauge redundancy, record accumulation, and geometric

reconstruction occur. A natural next question is whether these structures can be unified within a single variational object. This section develops the answer in two phases. §§12.1–12.5 propose a candidate VERSF master action and state its programmatic structure — renormalisation flow, fixed-point hierarchy, universality class, and central conjecture — addressing the open item flagged in §11.3 fourth (iii); the framing in those subsections is *programmatic*, with the forms stated as candidate first proposals and the central theorem stated as a conjecture. §§12.6–12.13 then supply the first concrete computational instances of that programme: the explicit block-fold RG flow with its non-trivial gauge fixed point (§12.6), first-pass estimates of the critical exponents (§12.7), the conservation-fixed closure-response kernel mapping ρ → Φ_{μν} (§§12.8–12.9), the constrained leading-order uniqueness of the local record-current functional C^{μν}[Φ] (§12.10), the structural decomposition of SU(3) × SU(2) × U(1) from $\mathscr{H}$_fold ≅ $\mathbb{C}^4$ (§12.11), the explicit Monte Carlo lattice programme (§12.12), and the first preliminary numerical diagnostics (§12.13). §12.14 collects the open items the calculational programme still faces.

12.1 Candidate Unified Action

The proposed master action decomposes over the 2D commitment interface Σ (Definition 4.1) and the emergent coarse-grained 4D bulk M:

S_VERSF = ∫_Σ [$\mathscr{L}$_fold + $\mathscr{L}$_closure + $\mathscr{L}$_gauge + $\mathscr{L}$_commit] d²σ + ∫_M [$\mathscr{L}$_record + $\mathscr{L}$_geom + $\mathscr{L}$_memory] √(−g) d⁴x.

Each Lagrangian density corresponds to a sector developed in §§3–10:

Interface (Σ) sector.

$\mathscr{L}$_fold = J_σ Σ_⟨ij⟩ (1 − σ$_i$σ$_j$) + J_ω Σ_⟨ij⟩ (1 − ω$_i$ω$_j$) [Ising-type orientation/parity couplings, §4.4] $\mathscr{L}$_closure = λ Σ_ℓ (1 − Re U_ℓ) [Wilson-type closure penalty, §4.4] $\mathscr{L}$_gauge = −(1/4g²) F_μν F^μν + J^μ A_μ [Maxwell from closure transport, §7] $\mathscr{L}$_commit = Σ_ℓ Θ($\mathcal{C}$_ℓ − $\mathcal{C}$*) Δ_ℓ [irreversible fold-formation operator, §5]

Bulk (M) sector.

$\mathscr{L}$_record = ½ ∇_μ ρ ∇^μ ρ − V(ρ) [kinetic + potential for record field, §§5, 9] $\mathscr{L}$_geom = (1/2κ)(R − 2Λ) + α Φ_μν T^μν [Einstein–Hilbert + tensorial coupling, §10] $\mathscr{L}$_memory = ½ ∫ dτ ρ(x, t) K_sel(τ) ρ(x, t − τ) [non-Markovian memory kernel, §5]

with the metric defined by g_{μν} = (1/λ_★) Φ_{μν} (Theorem 10.0) and the memory kernel by K_sel(τ) = cos(mτ)/(2πτ), m = C_m ξ⁻¹.

The substrate-to-bulk bridge is implicit in the structure: the interface fold dynamics generate the record source, and the record source generates gauge and geometric structure at coarse scale. Schematically,

S_VERSF = S_Σ[σ, ω, U, Θ] + S_M[ρ, Φ_μν, g_μν, A_μ, Ξ],

with Ξ the causal memory field of §5. The Lagrangians of the M-sector are not independent of those on Σ; they describe the coarse-grained image of Σ-dynamics on the emergent bulk. None of the bulk Lagrangians is fundamental — each is a Layer-4 effective description of substrate-level structural dynamics (see §11.3 sixth scope note).

12.2 Renormalisation Flow

Introducing a coarse-graining scale $b > 1$ (lattice spacing $a \to a' = ba$), the substrate parameters $\{J_\sigma, J_\omega, \lambda, g, \mathcal{C}^*, \kappa, \beta_\Xi\}$ acquire scale-dependent values along the renormalisation flow

$d \ln J_\sigma / d \ln b = \beta_{J_\sigma}$, $d \ln J_\omega / d \ln b = \beta_{J_\omega}$, $d g / d \ln b = \beta_g$, $d \lambda / d \ln b = \beta_\lambda$, $d \mathcal{C}^* / d \ln b = \beta_{\mathcal{C}^*}$, $d \kappa / d \ln b = \beta_\kappa$.

Specific β-functions are not derived here, but plausible first forms can be written. The Abelian gauge coupling is expected to follow a standard one-loop form modified by interface dynamics:

$$\beta_g = -(b_0 / 16\pi^2)\, g^3 + \eta_{\text{fold}}\, g,$$

where η_{fold} is an anomalous dimension induced by fold-interface transport. The commitment threshold is expected to satisfy

$$\beta_{\mathcal{C}^*} = (2 - \Delta_{\mathcal{C}^*})\, \mathcal{C}^* - \alpha_{\mathcal{C}}\, \lambda\, \mathcal{C}^*,$$

with $\Delta_{\mathcal{C}^*}$ the engineering dimension of $\mathcal{C}^*$. The record field scales as

$$\rho'(x) = b^{-\Delta_\rho}\, \rho(b^{-1}\, x), \quad \Delta_\rho = d - \theta,$$

where θ is a hyperscaling-violation exponent induced by the interface/bulk reconstruction. These are first-pass forms; their definitive derivation is open work and would require both an explicit choice of regulator on the substrate side and a derivation of the coarse-graining map from interface dynamics to bulk record dynamics.

12.3 Fixed-Point Structure

Four fixed points are anticipated along the RG flow:

(I) Void fixed point (UV boundary). $J_\sigma = J_\omega = \lambda = g = \rho = 0$. No folds, no loops, no topology, no physics. $\beta_i = 0$ trivially, but the fixed point is unstable once commitment perturbations appear. Interpretation: the Void is the zero-commitment ultraviolet boundary condition of the framework, not a vacuum *in* the framework.

(II) Fold / interface critical point. At $\mathcal{C}_\ell = \mathcal{C}^*$ ($\beta_{\mathcal{C}^*} = 0$) the coherence length ξ diverges. This is the transition where reversible fluctuations become irreversible folds. Fold formation is therefore a *critical phenomenon*, with diverging correlation length at the threshold — a structurally important consequence, since it places fold dynamics in the universality class of

continuous phase transitions and opens the formal study of fold ensembles to the standard apparatus of critical-phenomena analysis.

(III) Maxwell / continuum transport infrared fixed point. At large scales, $a \to 0$ and $U\_p \to \exp(ia^2 F\_\mu\nu)$, the Wilson action $S\_W \to \int F\_\mu\nu F^\mu\nu d^4x$, and the field equation $\partial\_\mu F^\mu\nu = \mu_0 J^\nu$ follows (the discrete-to-continuum calculation of §7). Maxwell theory is the Abelian infrared fixed point of closure transport.

(IV) Geometric / Einstein infrared fixed point. At still larger scales, $g\_\{\mu\nu\} = \Phi\_\{\mu\nu\}/\lambda\_\bigstar$ (Theorem 10.0) and Lovelock closure yields $G\_\{\mu\nu\} + \Lambda\, g\_\{\mu\nu\} = \kappa\, T\_\{\mu\nu\}$. Einstein dynamics is the tensorial infrared fixed point of accumulated record closure.

12.4 Universality Class

The VERSF universality class is hybrid: a 2D $\mathbb{Z}_2 \times \mathbb{Z}_2$ Ising-like fold lattice coupled to U(1) closure gauge transport, modulated by irreversible threshold dynamics, with record-memory bulk reconstruction. The principal exponents to be determined are:

- ν — coherence-length exponent at the fold / interface critical point (Fixed Point II);
- η — fold-correlation anomalous dimension;
- z — dynamic exponent relating spatial and temporal scaling;
- θ — hyperscaling-violation / depth-reconstruction exponent (entering Δ_ρ);
- ζ — memory-kernel exponent governing the long-time tail of K_sel.

The memory kernel $K\_sel(\tau) \sim \cos(m\tau)/\tau$ has algebraic decay $\tau^\{-1\}$, implying $\zeta = 1$: the temporal memory sector carries a non-Markovian universality signature distinguishing this class from Markovian critical systems. The remaining exponents are not yet derived from the substrate dynamics.

12.5 The Central Conjecture

The central mathematical target is the following:

Conjecture 12.1 (VERSF IR Convergence). Under finite distinguishability, local reversible pre-commitment dynamics, closure consistency, irreversible threshold firing, and coarse-grainability, the VERSF master action has an infrared fixed point whose Abelian sector is Maxwell transport and whose tensorial record sector is Einstein-type geometry. In compact form,

$S\_\text{VERSF} \text{—RG}\to S\_\text{Maxwell} + S\_\text{Einstein} + S\_\text{memory},$

or explicitly

$S\_\text{VERSF} \longrightarrow \int [-(1/4g^2)\, F\_\mu\nu\, F^\mu\nu + (1/2\kappa)(R - 2\Lambda) + \mathscr{L}\_\text{memory}]\, \sqrt{(-g)}\, d^4x.$

This is the mathematical target toward which the substrate-structural results of §§3–10 collectively point. Establishing the conjecture rigorously requires (i) explicit forms for the β-

functions of all running couplings derived from the substrate dynamics, (ii) a proof that the fixed-point structure (I)–(IV) actually closes (no other fixed points compete), (iii) explicit derivation of the universality-class exponents ν, η, z, θ, ζ from the cell-level dynamics of §4, and (iv) a treatment of the memory kernel under coarse-graining beyond the schematic $\zeta = 1$ form. These are natural next pieces of programme work.

The intended fixed-point picture is therefore clear: the Void is the zero-commitment ultraviolet boundary condition; the Fold is the critical commitment surface; Maxwell transport is the Abelian infrared fixed point of closure dynamics; Einstein geometry is the tensorial infrared fixed point of accumulated record reconstruction. The master action $S_$VERSF, with its honest set of open items, is what unifies them — *as a target rather than as a completed derivation*.

The remaining subsections of §12 give the master-action programme calculational form. §12.6 supplies the first computable RG flow on the minimal Abelian substrate action. §12.7 supplies first-pass estimates of the fold-transition critical exponents. §§12.8–12.9 develop the closure-response kernel that bridges record density to the rank-2 sector and derive its conservation-fixed form. §12.10 establishes a constrained leading-order uniqueness theorem for the local record-current functional $C^{\mu\nu}[\Phi]$ appearing in the master action's conservation-constraint term. §12.11 supplies the structural decomposition of SU(3) × SU(2) × U(1) from $\mathscr{H}_$fold $\cong \mathbb{C}^4$ that initiates the non-Abelian extension. §12.12 turns the block-fold RG into an explicit Monte Carlo recipe. §12.13 reports the first preliminary numerical diagnostics. §12.14 collects the open items the calculational programme still faces.

12.6 First Computable RG Flow

The schematic flows of §12.2 acquire concrete content when the block-fold map is evaluated on the minimal Abelian substrate action. Take

$$S\_\Sigma = J\_\sigma \Sigma\_\langle ij\rangle (1 - \sigma_i\sigma_j) + J\_\omega \Sigma\_\langle ij\rangle (1 - \omega_i\omega_j) + \lambda \Sigma\_p (1 - \mathrm{Re}\, U\_p)$$

as the minimal substrate action — the toy form of the transport action of §4.4 retained at leading order, prior to inclusion of the fold-formation threshold operator. Under a block-fold map B_b taking b^2 hexagonal cells of a region $R\_b \subset \Sigma$ into one effective cell, define the effective block variables by majority orientation, majority parity, and plaquette-averaged holonomy:

$$\sigma' I = sgn\, \Sigma\{i \in I\}\ \sigma_i,\ \omega' I = sgn\, \Sigma\{i \in I\}\ \omega_i,\ U' IJ = \prod\{\langle ij\rangle \in \Gamma\_IJ\}\ U_{ij},$$

where Γ_IJ denotes the path of links bridging block I and block J under the chosen block decomposition. The renormalised action is defined by partial tracing over sub-block degrees of freedom (the block-spin / block-fold formalism named in §12.2):

$$e^{-S'[\sigma', \omega', U']} = \Sigma\_\{\{\sigma, \omega\}: B\_b(\sigma, \omega, U) = (\sigma', \omega', U')\}\ e^{-S[\sigma, \omega, U]}.$$

To leading order around their fixed-point values, the Ising-like sectors obey the standard near-critical form

$dJ_\sigma / d\ln b = y_\sigma (J_\sigma - J_\sigma^*) + \mathcal{O}((J_\sigma - J_\sigma^*)^2)$, $dJ_\omega / d\ln b = y_\omega (J_\omega - J_\omega^*) + \mathcal{O}((J_\omega - J_\omega^*)^2)$,

with leading scaling dimensions y_σ, y_ω at the corresponding critical points (J_σ^*, J_ω^*) of the orientation and parity sectors. The Abelian closure coupling obeys the one-loop form

$dg / d\ln b = -(b_0 / 16\pi^2)\, g^3 + \eta_{fold}\, g$,

where the first term is the standard pure-gauge contribution (with b_0 a positive constant set by the closure-loop diagrams of the discrete dynamics) and the second term is the fold-induced anomalous dimension defined operationally through the rescaling

$U'_p = b^{-\eta_{fold}}\, U_p$

of the plaquette holonomy under B_b.

The non-trivial gauge fixed point of this flow satisfies

$g^{*2} = 16\pi^2\, \eta_{fold} / b_0$,

provided $b_0 > 0$ and $\eta_{fold} > 0$. The interpretation is direct: fold-induced anomalous scaling can stabilise a non-zero closure-transport fixed point rather than allowing the Abelian sector to flow trivially to either zero or infinity. Whether the substrate dynamics actually produce b_0, $\eta_{fold} > 0$ is a calculational question that the explicit block-fold map above makes well-posed.

Structural analogy with the Wilson–Fisher mechanism. The β-function above has the same mathematical structure as the $d = 4 - \varepsilon$ flow that produces the Wilson–Fisher fixed point (Wilson & Fisher, 1972): in $d = 4 - \varepsilon$ with engineering-dimension contribution, the renormalisation flow of a gauge coupling takes the form $\beta_g = (\varepsilon/2)\, g - (b_0 / 16\pi^2)\, g^3$, with a non-trivial fixed point at $g^{*2} = 8\pi^2\, \varepsilon / b_0$. The additive $\eta_{fold} \cdot g$ term in the VERSF β-function plays the same role as the $(\varepsilon/2)\, g$ term in the $d = 4 - \varepsilon$ flow, with $\eta_{fold} \leftrightarrow \varepsilon/2$ modulo normalisation. The η_{fold} term is therefore not an ad hoc addition to the standard one-loop β-function; it is structurally identical to the dimensional-counting term that produces Wilson–Fisher fixed points, with η_{fold} operating as an effective shift in the dimensional counting of g. The physical origin differs — $\eta_{fold} > 0$ here arises from the closure-loop-induced anomalous rescaling $U'_p = b^{-\eta_{fold}}\, U_p$ of the plaquette holonomy under B_b, not from a literal dimensional shift — but the mechanism by which a positive linear-in-g contribution stabilises a non-zero fixed point against the standard $-g^3$ flow is the same as the Wilson–Fisher mechanism.

This is the first concrete instance of the block-fold renormalisation programme called for by §12.2. The leading-order forms above can be extended systematically: higher-loop corrections to the gauge β-function, cross-couplings between the orientation/parity and gauge sectors mediated by the closure-penalty λ, and the running of the threshold $\mathcal{C}^*$ under B_b. Each is a natural next computation; the present formulation supplies a concrete starting point for them all.

12.7 First Estimate of Critical Exponents

The renormalisation flow of §12.6 reaches its first phenomenological output in the critical exponents of the fold transition at Fixed Point II of §12.3. We present first estimates at two levels: a baseline universality-class assignment from the structure of the $\mathbb{Z}_2 \times \mathbb{Z}_2$ fold sectors, and an emergent-depth correction from the interface-to-bulk reconstruction.

Fold-transition universality estimate. The fold transition is governed by the two coupled $\mathbb{Z}_2$ sectors (σ, ω) of Definition 4.1. The closure-penalty term λ Σ_p (1 − Re U_p) couples these sectors directly via the plaquette holonomy. At λ = 0 (the uncoupled baseline), the (σ, ω) sectors decouple into two independent 2D Ising systems; the standard 2D Ising exponents (Onsager, 1944; Kadanoff, 1966) then give

$\nu_0 = 1$, $\eta_0 = 1/4$, $z_0 \approx 2$.

At finite λ, the coupling between the two $\mathbb{Z}_2$ variables places the system in the Ashkin–Teller universality class (Ashkin & Teller, 1943) rather than the doubled-Ising class. The 2D Ashkin–Teller model has a critical line along which the exponents (ν, η) vary continuously with the four-spin coupling between the two $\mathbb{Z}_2$ variables. The doubled-Ising point is one endpoint of this Ashkin–Teller critical line; finite λ moves the system along the line and produces corrections to (ν_0, η_0) of the same parametric size as the gauge and memory corrections discussed below. We retain the doubled-Ising baseline as the first-pass estimate, with the understanding that the explicit λ-running of (ν, η) along the Ashkin–Teller critical line is one of the next computations the block-fold map B_b of §12.6 is set up to address.

Thus near the fold threshold, with reduced commitment parameter $t_{\mathcal{C}} = (\mathcal{C}_\ell - \mathcal{C}^*)/\mathcal{C}^*$,

$\xi \sim |t_{\mathcal{C}}|^{-1}$, $G(r) \sim (1/r^{1/4})\, e^{-r/\xi}$.

Gauge closure and memory effects deform these into corrected exponents $\nu = 1 + \delta\nu_{\text{closure}}$, $\eta = 1/4 + \delta\eta_{\text{closure}}$, $z = 2 + \delta z_{\text{memory}}$, with corrections that are not yet computed from substrate dynamics; the block-fold map B_b of §12.6 is the natural setting for their derivation. The memory exponent $\zeta = 1$ is fixed exactly by the algebraic τ^{-1} tail of the memory kernel $\cos(m\tau)/\tau$ already noted in §12.4.

Dimensional reconstruction from emergent depth. Because the physical bulk depth coordinate is *reconstructed* rather than fundamental — folds form on a two-dimensional interface (Definition 4.1) but the bulk record reconstruction supplies an emergent depth axis (§9.1) — the effective scaling dimension of the system differs from the lattice dimension on which the block-fold map operates. Let $d_\Sigma = 2$ be the interface dimension and d_{eff} be the effective scaling dimension. We define a *dimensional-reconstruction parameter* θ by $d_{\text{eff}} = d_\Sigma - \theta$. If the reconstructed depth contributes one effective dimension at large scale, then $d_{\text{eff}} \approx 3$, giving

$2 - \theta \approx 3$, hence $\theta \approx -1$.

A note on terminology. The relation $d_{\text{eff}} = d_\Sigma - \theta$ has the same formal structure as the hyperscaling-violation relation familiar from conventional condensed-matter contexts (where positive θ marks effective-dimension reduction under spatial coarse-graining). The physical

origin in VERSF is different. The block-fold map B_b of §12.6 operates on the 2D interface Σ; under spatial coarse-graining alone, d_Σ stays 2. The third effective dimension is *reconstructed* from the temporal sequence of fold-formation updates (§9.1), not from spatial coarse-graining. The shift $\theta \approx -1$ therefore counts dimensions added by temporal-to-spatial reconstruction, not dimensions effectively lost through anomalous spatial scaling. Calling this a "hyperscaling-violation exponent" would borrow the formal structure of the relation without the physics that gives it its usual content; we therefore use *dimensional-reconstruction parameter* and reserve "hyperscaling violation" for its conventional usage. The modified scaling relation

$$2 - \alpha = \nu(d_\Sigma - \theta),$$

with d_Σ the lattice dimension on which the block-fold map acts and θ the dimensional-reconstruction shift from the emergent-depth reconstruction, then gives $2 - \alpha \approx 3$, hence $\alpha \approx -1$.

Summary. The first-pass universality-class data for the fold transition is therefore

$$(\nu, \eta, z, \theta, \zeta, \alpha) \approx (1, 1/4, 2, -1, 1, -1).$$

This reduces the named-but-undetermined exponent programme of §12.4 to a sharper problem: starting from the Ising baseline and the emergent-depth estimate above, compute the corrections ($\delta\nu_{\text{closure}}$, $\delta\eta_{\text{closure}}$, δz_{memory}) and refine θ from the explicit block-fold map of §12.6.

12.8 The Closure-Response Kernel: Minimal Covariant Ansatz

The microscopic-to-geometric chain underpinning Conjecture 12.1 was assembled in earlier subsections: cell-level fold states (Definition 4.1) → threshold indicator χ_ℓ (§5) → record density ρ → rank-2 commitment field $\Phi_{\mu\nu}$ (Theorem 10.0) → metric $g_{\mu\nu} = \Phi_{\mu\nu}/\lambda_\star$ → Einstein dynamics. The structural object that bridges record density and the rank-2 sector — the arrow $\rho \to \Phi_{\mu\nu}$ — has the explicit linear form

$$\Phi_{\mu\nu}(x) = \int K_{\mu\nu}(x, x')\, \rho(x')\, d^4x',$$

where $K_{\mu\nu}(x, x')$ is the **closure-response kernel** induced by coarse-grained fold transport. The specific form of this kernel was not fixed at the level of §10 itself.

We propose as a first-pass model the minimal covariant ansatz

$$K_{\mu\nu}(x, x') = A\, g_{\mu\nu}\, G_m(x, x') + B\, \nabla_\mu \nabla_\nu\, G_m(x, x'),$$

where G_m is the retarded Green function of the massive record-response operator,

$$(\Box + m^2)\, G_m(x, x') = \delta^{(4)}(x - x'),$$

with mass parameter $m = C_m\, \xi^{-1}$ inherited from the κ-field of §5. This minimal ansatz is the most general covariant rank-2 kernel built from $g_{\mu\nu}$, $\nabla\mu$, *and a single propagator* G_m *at leading derivative order, and contains exactly two coefficients. The first term supplies the scalar*

trace response (the metric trace direction); the second supplies directional and tidal structure (the traceless rank-2 directions of the $\Phi\{\mu\nu\}$ field).

The two coefficients A and B are not free: conservation of the record current $\nabla^\mu \Phi_{\mu\nu} = 0$ imposes a relation between them, and the surviving response strength is then fixed by Newtonian matching. The next subsection carries out that derivation.

12.9 First Derivation of the Closure-Response Kernel

The previous subsection introduced the ansatz $K_{\mu\nu} = A\, g_{\mu\nu}\, G_m + B\, \nabla_\mu \nabla_\nu G_m$, leaving the two coefficients A, B to be determined by physical requirements. Conservation of the record current,

$$\nabla^\mu \Phi_{\mu\nu} = 0,$$

now allows the relation between A and B to be derived rather than postulated.

The conservation calculation in the flat low-curvature limit. Covariant derivatives reduce to partial derivatives, $\nabla_\mu \to \partial_\mu$, and the massive Green function G_m satisfies $(\Box + m^2)\, G_m = \delta^{(4)}(x - x')$. Taking the divergence of the kernel ansatz gives

$$\partial^\mu K_{\mu\nu} = A\, \partial_\nu G_m + B\, \partial^\mu \partial_\mu \partial_\nu G_m.$$

In the flat limit, partial derivatives commute, so $\partial^\mu \partial_\mu \partial_\nu G_m = \partial_\nu \Box G_m$. Using $\Box G_m = \delta^{(4)} - m^2 G_m$, the divergence becomes, away from the source,

$$\partial^\mu K_{\mu\nu} = (A - B\, m^2)\, \partial_\nu G_m.$$

The conservation constraint. For $\nabla^\mu \Phi_{\mu\nu} = 0$ to hold away from the source, the coefficient of $\partial_\nu G_m$ must vanish:

$A - B\, m^2 = 0$, hence $\boldsymbol{A = B\, m^2}$**.**

This is the first concrete derivation result of the kernel programme: conservation in the flat low-curvature limit forces a specific algebraic relation between the scalar and tensorial coefficients of the minimal covariant kernel. The two-coefficient ansatz of §12.8 collapses to a one-coefficient kernel.

A note on the source contact term. The conservation condition $A = B\, m^2$ eliminates the smooth (Green-function) part of $\partial^\mu K_{\mu\nu}$, but the contact-term contribution $B\, \partial_\nu \delta^{(4)}(x - x')$ from $\Box G_m = \delta^{(4)} - m^2 G_m$ survives. Retaining it:

$$\partial^\mu K_{\mu\nu}(x, x') = (A - B\, m^2)\, \partial_\nu G_m(x, x') + B\, \partial_\nu \delta^{(4)}(x - x').$$

With $A = B\, m^2$, the smooth part vanishes; the contact term remains. Integrating against the source $\rho(x')$ — which is how $\Phi_{\mu\nu}$ is actually built — gives

$\nabla^\mu \Phi_{\mu\nu}(x) = -\lambda_K B \partial_\nu \rho(x)$,

so $\nabla^\mu \Phi_{\mu\nu}$ vanishes in source-free regions ($\rho = 0$) but not where ρ is present. This is the natural stress-energy structure: the record density ρ acts as a covariant source for the divergence of the rank-2 commitment field, mirroring the way energy-momentum is conserved in matter-free regions and sourced by the matter stress tensor where matter is present. The conservation-fixed kernel is therefore *source-covariant* rather than absolutely conserved; the role of $\Phi_{\mu\nu}$ as the gravitational object that ρ sources is what gives $\nabla^\mu \Phi_{\mu\nu} = -\lambda_K B \partial_\nu \rho$ its physical reading.

The conservation-fixed kernel. Substituting $A = B\, m^2$ back and absorbing B into a single response strength λ_K, the kernel takes the form

$$K_{\mu\nu}(x, x') = \lambda_K \left[m^2 g_{\mu\nu}\, G_m(x, x') + \nabla_\mu \nabla_\nu G_m(x, x')\right],$$

and the rank-2 commitment field becomes

$$\Phi_{\mu\nu}(x) = \lambda_K \int \left[m^2 g_{\mu\nu}\, G_m + \nabla_\mu \nabla_\nu G_m\right] \rho(x')\, d^4x'.$$

The bridge $\rho \to \Phi_{\mu\nu}$ is now mediated by a *derived* conserved rank-2 Green-function kernel rather than by an undefined response map.

Fixing the response strength. The single remaining coefficient λ_K is calibrated by matching to the Newtonian limit. In companion programme work on fold density gradients, the trace of $\Phi_{\mu\nu}$ in the weak-field limit reduces to the scalar bound-information potential satisfying $\nabla^2 \Phi_{bound} = 4\pi \lambda c^2 \xi \rho_{bound}$, where λ is the substrate coupling, c the speed of light, ξ the coherence scale, and ρ_{bound} the bound-information density. Taking the trace $\Phi \equiv g^{\mu\nu} \Phi_{\mu\nu}$ of the rank-2 field and demanding it reproduce $\nabla^2 \Phi_{bound}$ in the $m \to 0$ limit fixes λ_K in terms of (λ, c, ξ).

12.10 Constrained Uniqueness of the Record-Current Functional

§§12.8–12.9 established the closure-response kernel that maps the scalar record density ρ to the rank-2 commitment field $\Phi_{\mu\nu}$: $\Phi_{\mu\nu}(x) = \int K_{\mu\nu}(x, x')\, \rho(x')\, d^4x'$ with $K_{\mu\nu} = \lambda_K [m^2 g_{\mu\nu} G_m + \nabla\mu\, \nabla\nu\, G_m]$. *The kernel governs *how $\Phi_{\mu\nu}$ is built from ρ*. A distinct rank-2 object governs *how the record content carried by $\Phi_{\mu\nu}$ flows**: the local record-current functional $C^{\mu\nu}[\Phi]$. This subsection establishes its functional form by a constrained-uniqueness argument paralleling that of §§12.8–12.9 but with a richer constraint structure.

The object and its role. The master-action programme includes a conservation-constraint term

$$\lambda_\mu \left(\nabla_\nu C^{\mu\nu}[\Phi] - \mathcal{S}^\mu[\Phi]\right),$$

where λ_μ is a Lagrange-multiplier vector field whose variation enforces $\nabla_\nu C^{\mu\nu} = \mathcal{S}^\mu$ at every point, and $\mathcal{S}^\mu$ is the commitment-density vector — the rank-1 divergence projection of the rank-2 commitment-density functional $\mathcal{S}^{\mu\nu}[\Phi]$ derived elsewhere in the programme via

the TPB-entropy structure. C^{μν}[Φ] is the local rank-2 record-current functional: physically, the rate at which record-content flows through each spacetime point; mathematically, the object whose divergence is forced by variation of λ_μ to equal the commitment-density vector.

Two distinctions from §§12.8–12.9 are worth keeping in view. *Locality:* K_{μν}(x, x') is a non-local Green-function kernel; C^{μν}Φ is a local functional evaluated pointwise. *Role:* K_{μν} bridges ρ → Φ_{μν}; C^{μν} bridges Φ_{μν} → ∇_ν C^{μν} = $\mathcal{S}$^μ. Both are rank-2 symmetric tensors derived by constrained uniqueness — the family resemblance is real, but the architecture is distinct.

Order-matching across the conservation identity. The leading-order C^{μν} derived in this subsection is *linear* in Φ, while the leading-order form of $\mathcal{S}$^μ = ∇_ν $\mathcal{S}$^{μν} inherited from the commitment-density structure of §5 (closed by the TPB-entropy programme work) is *cubic* in Φ modulo TPB-dependence. For the conservation identity ∇_ν C^{μν} = $\mathcal{S}$^μ to hold as a leading-order *kinematic identity*, the TPB[Φ] functional must carry a |Φ|² scaling at leading order, absorbing the cube — i.e., TPB[Φ] ~ |Φ|² × (substrate-scale factors). This is a corpus-level consistency requirement on the TPB scaling structure rather than a hole in the present derivation: the constraints (K1)–(K6) act on the form of C^{μν} at the linear level and are independent of the resolution. Should the expected TPB scaling fail, the conservation identity would instead define a non-trivial constraint surface in configuration space rather than a kinematic identity — substantive but admissible, and not affecting the leading-order form derived here.

Regime. The analysis is *continuum-limit*: the integrals over d⁴x, the smooth metric g_{μν}, the covariant derivative ∇, and the EFT power-counting in (∂/Λ_sub) are all continuum-limit constructs, correct in the regime where the substrate has been smoothed over many ticks and many cells but not at the substrate scale itself. The theorem below is a claim about the continuum-limit record current, not about a hypothetical substrate-level current — consistent with the master-action framing of §§12.1–12.5.

Candidate space. Under (i) Φ_{μν} a symmetric rank-2 tensor and (ii) C^{μν}[Φ] a local covariant functional of Φ_{μν}, g_{μν}, the substrate-emergent vector U^μ, the curvature R^{μν}_{αβ}, and ∇, the most general leading-order form is

$$C^{\mu\nu}[\Phi] = a\,\Phi^{\mu\nu} + b\,g^{\mu\nu}\,\Phi + c\,\nabla^{(\mu}V^{\nu)}[\Phi] + d\,\Phi^{\mu\alpha}\,\Phi^{\nu}{}_{\alpha} + e\,\Phi^{\mu\nu}\,|\Phi|^2 + f\,R^{\mu\nu}\,\Phi + h\,R\,\Phi^{\mu\nu} + j\,\Phi\,U^{\mu}U^{\nu} + k\,\Phi^{(\mu}{}_{\alpha}\,U^{\nu)}\,U^{\alpha} + \cdots$$

The terms group into five structural classes — linear field, gradient, bilinear, curvature, and substrate-vector — with trailing higher-order contributions. The candidate space is the admissible coefficient tuples modulo the six physical constraints below.

Six physical constraints.

- **(K1) Conservation compatibility.** ∇_ν C^{μν} must equal the commitment-density vector $\mathcal{S}$^μ supplied by the master action, by structure of the λ_μ-constraint term.
- **(K2) No pure-gauge redundancy.** Among representatives sharing the same divergence, the canonical form is the one of lowest derivative order with the fewest independent

terms. (K2) is a parameterisation choice fixing the canonical representative within each gauge-equivalence class; it does not exclude any physical record current.

- **(K3) Tensor symmetry.** C^{μν} = C^{νμ}. The rank-2 record current sources rank-2 stress-energy via the constraint contribution to T_{μν}, and physical stress-energy is symmetric.
- **(K4) Additivity over disjoint supports.** C^{μν}_{A∪B} = C^{μν}_A + C^{μν}_B when supports are disjoint. This is the substrate-level statement of region-wise independence. Crucially, (K4) does not exclude entangled configurations — non-local correlations live within Φ itself, not in the functional dependence of C^{μν} on Φ.
- **(K5) Scalar reduction at divergence level.** The divergence ∇*v C^{μν} must reduce in the trace-pure limit Φ*{μν} → ¼ g_{μν} Φ to the scalar record-current vector of the kinematic-conservation strand of the VERSF programme — matched at the rank-1 (vector) projection where the tensor and scalar formulations share rank.
- **(K6) Stress-energy consistency.** The constraint contribution to T_{μν} arising from variation of λ_μ(∇_ν C^{μν} − 𝒮^μ) with respect to g^{μν} must be consistent with the gravitational response of §10 (and the convergent companion programme work on fold-density-gradient gravity).

(K1) and (K6) bind C^{μν} to the rest of the programme; (K2)–(K5) are internal to the functional itself.

Theorem 12.2 (Leading-Order Uniqueness of C^{μν}[Φ]). *Under (K1)–(K6) and at leading order in the substrate expansion in (Φ/Φ_sub), (∂/Λ_sub), and (Rℓ_sub²), the rank-2 record-current functional is forced to*

C^{μν}[Φ] = a Φ^{μν} + b g^{μν} Φ,

with a and b dimensional constants set by substrate-scale physics. All other coefficients (c, d, e, f, h, j, k, ...) in the candidate space are eliminated or absorbed at leading order.

The methodology is standard EFT operator selection (Weinberg, 1995, 2016; Burgess, 2007), with Lovelock's theorem (1971) as the canonical analogue: under general covariance, locality, and low-derivative ordering, the gravitational sector is forced to Einstein–Hilbert; here under (K1)–(K6) and substrate ordering, the constitutive record-current sector is forced to the two-coefficient form. The closest external methodological precedent applied to a record-density-like source is Donoghue's EFT treatment of gravity (1994). The present paper does for the constitutive sector of the master action what Lovelock did for the geometric sector of general relativity.

Term-by-term elimination (compact).

- *aΦ^{μν}, bg^{μν}Φ — survive.* Linear in Φ, manifestly symmetric, local, additive. Divergences (a∇_ν Φ^{μν}, b∇^μΦ) are non-trivial and reduce correctly under (K5) to the leading α∇^μΦ structure of the scalar form. Both satisfy (K1)–(K5); (K6) constrains their relative weighting but eliminates neither.

- *$c\nabla^{(\mu} V^{\nu)}[\Phi]$ — parametrically suppressed.* The gradient term carries one extra derivative relative to the linear terms; its divergence contains $\Box\Phi$-type structures rather than the single-derivative $\nabla^\mu\Phi$ structure. Suppressed by (∂/Λ_{sub}) at leading order in the EFT power-counting.
- *$d\Phi^{\mu\alpha}\Phi^\nu{}_\alpha$, $e\Phi^{\mu\nu}|\Phi|^2$ — parametrically suppressed.* Bilinear-in-Φ terms carry an extra factor of (Φ/Φ_{sub}) relative to linear terms. Symmetric, local, and pointwise-additive under disjoint supports — they do not violate (K1)–(K4); their elimination is by substrate-scale suppression in the weak-field regime $\Phi \ll \Phi_{sub}$.
- *$fR^{\mu\nu}\Phi$, $hR\Phi^{\mu\nu}$ — parametrically suppressed.* Curvature-coupled terms carry an extra factor of $(R\ell_{sub}^2)$ in the regime where the master-action programme applies. Symmetric, local, and additive; suppression is by curvature scale.
- *$j\Phi U^\mu U^\nu$, $k\Phi^{(\mu}{}_\alpha U^{\nu)} U^\alpha$ — structurally eliminated.* The substrate-vector terms depend explicitly on the substrate-emergent vector U^μ; any explicit U-dependence in the leading-order $C^{\mu\nu}$ would produce observable preferred-frame effects, violating the empirical Lorentz invariance that the master action is required to reproduce. These terms vanish *exactly* in the exact emergent-Lorentz limit and reappear only at scales where Lorentz emergence is incomplete — a qualitatively different category of correction from (c, d, e, f, h).
- *Higher-order terms.* Cubic and higher in Φ, higher derivatives, products of curvature with bilinears — all suppressed by combinations of $(\Phi/\Phi_{sub})^n$, $(\partial/\Lambda_{sub})^n$, and $(R\ell_{sub}^2)^n$ at leading order.

Two mechanisms of exclusion. The eliminations above come in two qualitatively different categories. *Structural elimination*: j and k vanish exactly in the exact emergent-Lorentz limit, structurally absent at leading order in the emergent-Lorentz regime. *Parametric suppression*: c, d, e, f, h are non-zero in principle but suppressed by powers of substrate-scale parameters; they reappear systematically at subleading orders in the EFT expansion. The distinction matters because structurally forbidden operators are absent at all scales, while parametrically suppressed operators contribute to standard subleading corrections at every emergent-Lorentz scale.

Trace / trace-free decomposition. The two-coefficient form admits a cleaner parameterisation. Any symmetric rank-2 linear-in-Φ tensor decomposes uniquely into trace-free and trace parts:

$$C^{\mu\nu}[\Phi] = \tilde{a}\,(\Phi^{\mu\nu} - \tfrac{1}{4} g^{\mu\nu}\,\Phi) + \tilde{b}\, g^{\mu\nu}\,\Phi,$$

with $\tilde{a} = a$ and $\tilde{b} = a/4 + b$. The trace-free coefficient $\tilde{a}$ and the trace coefficient $\tilde{b}$ are physically independent: each parameterises a distinct sector of $C^{\mu\nu}$.

In this basis, (K5) fixes $\tilde{b}$ directly. The explicit calculation is straightforward: from the original parameterisation, the divergence is $\nabla_\nu(a\,\Phi^{\mu\nu} + b\, g^{\mu\nu}\,\Phi) = a\,\nabla_\nu\,\Phi^{\mu\nu} + b\,\nabla^\mu\,\Phi$. In the trace-pure limit $\Phi^{\mu\nu} \to \tfrac{1}{4} g^{\mu\nu}\,\Phi$, the first term reduces as $\nabla_\nu(\tfrac{1}{4} g^{\mu\nu}\,\Phi) = \tfrac{1}{4}\,\nabla^\mu\,\Phi$, giving

$$\nabla_\nu\, C^{\mu\nu}|_{\text{trace-pure}} = (a/4 + b)\,\nabla^\mu\,\Phi = \tilde{b}\cdot\nabla^\mu\,\Phi,$$

which matches the leading $\alpha\, \nabla^\mu \Phi$ coefficient of the kinematic-conservation scalar form. (K5) therefore imposes $\tilde{b} = \alpha_{\text{kinematic}}$ (modulo conventions). Then (K6) fixes the relation between $\tilde{a}$ and $\tilde{b}$ via stress-energy matching against the §10 gravitational response. Together, (K5) and (K6) reduce the two-parameter family to a single substrate-scale parameter.

Physically, $\tilde{a}$ measures how strongly the record current carries the field's anisotropic (trace-free) tensor content — the part that sources gravitational tensor modes and anisotropic stress. $\tilde{b}$ measures how strongly it carries conformal (trace) content — scale-dependent record content rather than directional. The two together specify how the substrate's record-bearing capacity is partitioned between anisotropic and conformal channels.

The (K6) matching condition, more concretely. Variation of the constraint sector $\int d^4x\, \sqrt{(-g)}\, \lambda_\mu (a\, \nabla_\nu \Phi^{\mu\nu} + b\, \nabla^\mu \Phi - \mathcal{S}^\mu)$ with respect to $g^{\mu\nu}$ produces the stress-energy contribution $T^{(C)}{}_{\mu\nu} = (-2/\sqrt{(-g)})\, \delta S_C/\delta g^{\mu\nu}$. Three sources contribute: the $\sqrt{(-g)}$ measure, the metric-dependence of the connection coefficients in ∇_ν acting on $\Phi^{\mu\nu}$, and the index-raising in $\nabla^\mu = g^{\mu\alpha}\, \nabla_\alpha$. Working through the standard variation (Christoffel variation $\delta\Gamma^\lambda{}_{\mu\nu}$, integration by parts, $\delta g^{\mu\nu} = -g^{\mu\alpha}\, g^{\nu\beta}\, \delta g_{\alpha\beta}$), the contribution decomposes into trace-free and trace tensor structures with coefficients linear in a and b respectively:

$$T^{(C)}{}_{\mu\nu} = a \cdot \mathcal{T}^{(TF)}{}_{\mu\nu}[\lambda, \Phi] + b \cdot \mathcal{T}^{(\mathrm{Tr})}{}_{\mu\nu}[\lambda, \Phi] + (\text{metric-projected trace contributions}).$$

The two structures are *linearly independent* — neither can be transformed into the other by index relabelling or metric contraction — so a and b couple to physically distinct gravitational sources. Matching against the independently derived rank-2 gravitational response of §10 (and the convergent companion programme work on fold-density-gradient gravity) gives a single algebraic relation

$$f(a, b) := \alpha\, b - \beta \cdot a \cdot \mathscr{R}[\Phi] = 0,$$

where α, β are the trace-free and trace coefficients of the §10 response and $\mathscr{R}[\Phi]$ is a substrate-dependent ratio fixed by on-shell evaluation. This reduces the (a, b) plane to a one-dimensional submanifold. Explicit numerical determination of α, β, and $\mathscr{R}[\Phi]$ requires joint analysis with the §10 / fold-density-gradients construction; the present subsection identifies the form of the matching condition and shows the calculation is well-posed.

What this gives the master-action programme. With the closure-response kernel of §§12.8–12.9 fixing how $\Phi_{\mu\nu}$ is built from ρ, and with $C^{\mu\nu}[\Phi] = a\, \Phi^{\mu\nu} + b\, g^{\mu\nu}\, \Phi$ fixing how the record content carried by $\Phi_{\mu\nu}$ flows, the constitutive sector of the master action — the two functional inputs that distinguish the VERSF master action from a generic rank-2 EFT — is closed at leading order. Both the commitment-density functional (closed by the TPB-entropy structure elsewhere in the programme) and the record-current functional (closed by Theorem 12.2 here) are now derived rather than postulated. The remaining content of the master action — kinetic, mass, and Einstein–Hilbert sectors — is inherited from the standard variational form for rank-2 tensor matter in curved spacetime. Conjecture 12.1's strengthened form is now a claim about a single specific theory rather than a family indexed by free constitutive functionals.

Three caveats. (i) Theorem 12.2 is a *constrained leading-order* uniqueness result in the EFT sense; subleading corrections from parametrically suppressed terms exist but do not affect the leading-order theory. (ii) The dimensional constants a, b are forced to be substrate-scale but are not derived from first principles — their values require additional substrate-level analysis or empirical matching. (iii) The decisive $\lambda^* \neq 0$ lattice test of §12.12 and the closure of the four-fixed-point structure of §12.3 remain open; Theorem 12.2 closes one constitutive functional, not the full master-action programme.

12.11 Non-Abelian Closure from $\mathbb{C}^4$

The Abelian sector of the master-action programme uses link variables $U_{ij} \in U(1)$. The strengthened form of Conjecture 12.1 calls for the non-Abelian extension $U_{ij} \in G$ with $G = SU(3) \times SU(2) \times U(1)$. The question is whether G can be derived from the substrate structure rather than imposed as an external input. This subsection presents the structural decomposition that initiates that derivation.

The per-fold Hilbert space established in §4.5 has dimension four: $\mathscr{H}\_\text{fold} \cong \mathbb{C}^4$. A natural decomposition consistent with the fold's internal structure is

$$\mathbb{C}^4 = \mathbb{C}^3 \oplus \mathbb{C}^1,$$

separating an active three-dimensional subspace from a one-dimensional residual phase. The natural unitary automorphism group preserving this decomposition is $U(3) \times U(1)$. Since $U(3) \cong (SU(3) \times U(1)) / \mathbb{Z}_3$, the colour-like SU(3) sector arises from transformations on the three-dimensional active subspace, while a residual Abelian phase supplies a U(1)-type channel.

The remaining SU(2) sector arises from the reversible binary directionality internal to each fold. The four-state basis is $|b, d\rangle$ with $b \in \{0, 1\}$ and $d \in \{+, -\}$; transformations preserving the binary reversible directionality act on the two-dimensional directional subspace spanned by $\{|\cdot, +\rangle, |\cdot, -\rangle\}$ as

$U\_\text{directional} = \exp(i\, \theta\_a\, \sigma\_a)$, $\sigma\_a \in su(2)$.

Combining these observations, the internal closure automorphism structure has the schematic decomposition

$\mathrm{Aut}(\mathscr{H}\_\text{fold}) \supset SU(3) \times SU(2) \times U(1)$,

containing the Standard Model gauge group as a subgroup of the natural automorphism structure of the per-fold Hilbert space.

Caveat on the subgroup structure. The structural observation above identifies $SU(3) \times SU(2) \times U(1)$ as a *named target* arising from the $\mathbb{C}^3 \oplus \mathbb{C}^1$ split and the $\{b, d\}$ basis, but the realised group structure within $\mathrm{Aut}(\mathscr{H}\_\text{fold}) = U(4) \supset SU(4)$ is more nuanced than a clean direct product. The d-index SU(2) acting on $\{|\cdot, +\rangle, |\cdot, -\rangle\}$ does not preserve the $\mathbb{C}^3 \oplus \mathbb{C}^1$ split of the b-index decomposition — the SU(2) action mixes states across the active/residual boundary in general —

so the SU(3) and SU(2) factors as identified above do not commute as actions on $\mathscr{H}$_fold, and SU(3) × SU(2) × U(1) is not realised as a clean direct-product subgroup of SU(4). The natural maximal-subgroup decomposition of SU(4) is instead the *nested* chain

$$SU(4) \supset SU(3) \times U(1)_1 \supset SU(2) \times U(1)_2 \times U(1)_1,$$

where the SU(3) acts on the active $\mathbb{C}^3$ via the b-index block decomposition, the $U(1)_1$ acts on the residual $\mathbb{C}^1$, and the SU(2) factor sits *within* SU(3) (via a further $\mathbb{C}^2 \oplus \mathbb{C}^1$ block decomposition of the active subspace) rather than as an independent factor commuting with it. The Standard Model gauge group's apparent direct-product form at the IR scale must therefore either arise as an effective IR description of the nested substrate structure, or be realised by additional closure-transport-sector structure that promotes the nested chain to an effective direct product at low energies. This is one of the substantive items the non-Abelian uniqueness programme work needs to address, alongside the uniqueness, admissibility, and chirality-selection questions named below.

This is a *structural* observation, not a *derivation*: it shows that G = SU(3) × SU(2) × U(1) is a *natural named target* arising from the $\mathbb{C}^3 \oplus \mathbb{C}^1$ decomposition and the $\{b, d\}$ basis, but it does not yet show that G is *uniquely* selected as the closure automorphism group, nor that it is realised as a direct-product subgroup rather than the nested chain identified above. The latter requires showing that admissibility, chirality, and closure sufficiency together rule out alternative subgroups (e.g. SU(4), SO(4), USp(4), etc.) that would otherwise be candidates, *and* that the closure-transport sector promotes the nested-chain structure to an effective direct product. This is the central task of the non-Abelian programme — taken up in companion VERSF programme work on the non-Abelian gauge algebra and on Abelian uniqueness and chirality selection, where uniqueness is addressed through admissibility-counting arguments and chirality-selection mechanisms.

With this decomposition in place, the non-Abelian extension of the Wilson construction of §7 proceeds in the standard way: path-ordered plaquette holonomies $U_p = \mathcal{P} \prod_{\ell \in \partial p} U_\ell$ with $U_{ij} \in G$, the Wilson action $S^G_W = \beta \Sigma_p (1 - (1/N) \mathrm{Re\ Tr}\ U_p)$ with N the dimension of the fundamental representation, and the continuum limit yielding the Yang–Mills action with structure-constant terms $F^a_{\mu\nu} = \partial_\mu A^a_\nu - \partial_\nu A^a_\mu + f^a_{bc} A^b_\mu A^c_\nu$ in the field strength. The strengthened form of Conjecture 12.1,

$$S_{\mathrm{VERSF}} \xrightarrow{\mathrm{RG}} S_{\mathrm{YM}} + S_{\mathrm{Einstein}} + S_{\mathrm{memory}},$$

then identifies the IR limit as Standard Model gauge dynamics plus Einstein gravity plus non-Markovian memory.

12.12 First Explicit Lattice Computation

The analytic block-fold RG flow of §12.6 supplies leading-order forms for the running couplings and identifies a candidate non-trivial gauge fixed point $g_*^2 = 16\pi^2\, \eta_{\mathrm{fold}} / b_0$. The first-pass critical-exponent estimates of §12.7 inherit from the doubled $\mathbb{Z}_2 \times \mathbb{Z}_2$ Ising baseline and the emergent-depth hyperscaling. To go beyond the leading-order forms — to obtain the explicit

functional forms F_σ, F_ω, F_λ of the running couplings, to verify the fixed point exists at finite coupling rather than only at the linearised level, and to refine the §12.7 critical exponents directly from the lattice flow — the next calculational step is a direct numerical evaluation of the block-fold map on a finite hexagonal lattice.

The partition function and the block-fold map. Begin with the partition function of the minimal Abelian substrate action of §12.6:

$$Z[J\_\sigma, J\_\omega, \lambda] = \Sigma\_{\{\sigma, \omega\}} \int \prod\_{\langle ij \rangle} \mathrm{d}U_{ij} \exp[-S\_\Sigma].$$

For a block I containing b^2 hexagonal cells, the block-fold variables of §12.6 are $\sigma' I = sgn\, \Sigma\{i \in I\}\ \sigma_i$, $\omega' I = sgn\, \Sigma\{i \in I\}\ \omega_i$, $U' I\!I = \prod\{\langle ij \rangle \in \Gamma\_\{IJ\}\}\ U_{ij}$. The renormalised action S' on the block lattice is defined by the constrained partial trace

$$e^{-S'[\sigma', \omega', U']} = \Sigma\_{\sigma, \omega} \int \mathrm{d}U\ \delta[B\_b(\sigma, \omega, U) - (\sigma', \omega', U')]\ e^{-S[\sigma, \omega, U]}.$$

Operator-basis matching. To obtain the first computable approximation, expand S' in the same operator basis as S:

$$S' = J'\sigma\, \Sigma\{\langle IJ \rangle\}\ (1 - \sigma'\_I\, \sigma'\_J) + J'\omega\, \Sigma\{\langle IJ \rangle\}\ (1 - \omega'\_I\, \omega'\_J) + \lambda'\, \Sigma\_P\ (1 - \mathrm{Re}\, U'\_P) + \cdots .$$

The trailing $\cdots$ denotes operators generated by the block-fold map that are not present in the bare action — systematically constructed multi-spin and higher-loop terms whose suppression is checked numerically (operator-basis truncation is an explicit, testable approximation). The running couplings J'_σ, J'_ω, λ' are extracted by matching expectation values of the same operators computed under S and under S':

$$\langle \sigma' I\, \sigma' J \rangle\{S'\} = \langle sgn(\Sigma\{i \in I\}\ \sigma_i) \cdot \mathrm{sgn}(\Sigma\_\{j \in J\}\ \sigma_j) \rangle\_S,$$

$$\langle \omega' I\, \omega' J \rangle\{S'\} = \langle sgn(\Sigma\{i \in I\}\ \omega_i) \cdot \mathrm{sgn}(\Sigma\_\{j \in J\}\ \omega_j) \rangle\_S,$$

$$\langle \mathrm{Re}\, U' P \rangle\{S'\} = \langle \mathrm{Re} \prod\_\{p \in P\}\ U\_p \rangle\_S.$$

Solving these matching conditions gives the running couplings as concrete functions of the bare couplings: $J'\_\sigma = F\_\sigma(J\_\sigma, \lambda)$, $J'\_\omega = F\_\omega(J\_\omega, \lambda)$, $\lambda' = F\_\lambda(\lambda, J\_\sigma, J\_\omega)$. These functions replace the schematic β-functions of §12.2 with concrete numerical objects extractable from the lattice.

Monte Carlo recipe. The first explicit numerical computation of the block-fold RG flow runs in six steps: (1) generate a finite hexagonal lattice of cells, with chosen $L \times L$ cell count and block factor b; (2) initialise $\sigma_i, \omega_i \in \{\pm 1\}$ on cells and $U_{ij} = \exp(i\theta_{ij})$ on edges; (3) Monte Carlo sample the partition function using S_Σ (standard Metropolis or heat-bath updates); (4) apply B_b to obtain $(\sigma'\_I, \omega'\_I, U'\_{IJ})$ on the block lattice; (5) measure $(J'\_\sigma, J'\_\omega, \lambda')$ from the matching expectation values; (6) iterate, feeding the measured couplings as new bare couplings at scale b and tracking the trajectory in coupling space. Standard finite-size scaling and finite-block-factor analysis applies.

Fixed points and critical exponents. A fixed point of the flow satisfies $J'\sigma = J\_\sigma, J'\omega = J\_\omega, \lambda' = \lambda$. *Linearising the flow around a fixed point yields the stability matrix* $M\{ab\} = \partial g'a / \partial g\_b |\{g = g^*\}$ with $g\_a = (J\_\sigma, J\_\omega, \lambda)$. Diagonalising M gives eigenvalues Λ_a and scaling dimensions $y\_a = \ln \Lambda\_a / \ln b$, with $\nu = 1 / y\_t$ (y_t the scaling dimension of the relevant operator at the fixed point). The corrections ($\delta\nu$_closure, $\delta\eta$_closure, δz_memory) of §12.7, left undetermined in the analytic treatment, emerge as concrete numerical outputs.

The decisive numerical test. The key result to look for is whether the block-fold map generates a stable interacting fixed point with non-zero closure coupling:

$\lambda \neq 0.*$

If it does, the analytic conjecture of §12.6 is confirmed by direct calculation: the non-trivial gauge fixed point exists at finite coupling and is reached under RG flow from a finite domain of initial conditions. Conjecture 12.1 then strengthens from a programmatic target into a numerically confirmed claim about the long-distance behaviour of the closure substrate:

Maxwell-like transport is not merely imposed on the interface; it appears as the *infrared fixed point of the lattice closure dynamics*.

If by contrast the flow drives $\lambda \to 0$ (the free Gaussian fixed point of §12.3, Fixed Point I) or $\lambda \to \infty$ (strong-coupling confinement), the analytic conjecture would need revision: either the operator-basis truncation is incomplete, or the substrate dynamics do not produce η_fold > 0 as required for the §12.6 fixed point to exist, or the structure of the block-fold map needs refinement. Either outcome is informative.

12.13 First Computational Diagnostics

The renormalisation-flow programme of §§12.2–12.11 is not intended only as a formal apparatus. The substrate action of §12.6 can be implemented numerically on finite lattices, allowing the first explicit tests of whether fold criticality and closure transport exhibit the anticipated co-emergent behaviour. This subsection reports two preliminary computational diagnostics — a baseline fold-sector RG check and a coupled fold-closure simulation — that establish the first empirical handles on the master-action programme.

Fold-sector RG diagnostic. As a first baseline test, the fold sector was simulated independently on the adjacency graph corresponding to hexagonal cells. The centres of hexagonal cells form a triangular lattice, so the fold variables $\sigma_i \in \{\pm 1\}$ were placed on a periodic triangular lattice with six nearest neighbours per site. The minimal fold action was taken as $S\_\text{fold} = J \Sigma\_\langle ij \rangle (1 - \sigma_i\sigma_j)$, equivalent up to a constant shift to the standard ferromagnetic Ising form. A Wolff-cluster Monte Carlo update was used near criticality to avoid critical slowing down. One-step block-fold coarse-graining was performed using majority blocking on 2 × 2 regions, producing an effective blocked coupling J'.

The resulting RG map showed strong flow toward larger effective coupling once the fold coupling approached the triangular-lattice critical baseline

$J\_c = (1/4) \ln 3 \approx 0.27465$.

The measured blocked coupling satisfied $J' > J$ above the transition region, indicating flow toward an ordered infrared phase — the standard signature of 2D Ising criticality on the triangular lattice. This supplies the first explicit computational evidence that the fold sector possesses a genuine critical transition on the substrate adjacency lattice rather than functioning only as a conceptual structural layer.

Limitations: only the $\mathbb{Z}_2$ orientation sector was included (the parity variable ω_i was held fixed), and no U(1) closure-holonomy dynamics were yet coupled to the fold variables. The next step is the coupled fold-closure simulation below.

Coupled fold-closure dynamics on hexagonal-cell adjacency. A second computation implemented coupled fold and closure dynamics on the correct six-neighbour adjacency graph. The substrate variables were fold variables $\sigma_i, \omega_i \in \{-1, +1\}$ on cells, and compact closure phases $\theta\_f \in [-\pi, \pi]$ attached to elementary triangular closure patches of the dual triangular lattice. The coupled substrate energy was

$E = E\_\text{fold} + E\_\text{closure} + E\_\text{coupling}$, $E\_\text{fold} = -J \Sigma\_\langle ij \rangle (\sigma_i \sigma_j + \omega_i \omega_j)$, $E\_\text{closure} = -\beta \Sigma\_f \cos \theta\_f$, $E\_\text{coupling} = -\gamma \Sigma\_f q\_f \cos \theta\_f$,

with $q\_f = (1/3)(q\_i + q\_j + q\_k)$ and $q\_i = \sigma_i \omega_i$ the local fold-coherence variable on each triangular closure face. Local Metropolis updates were applied independently to (σ, ω) and θ_f. The principal observables measured were $\langle|\sigma|\rangle$, $\langle|\omega|\rangle$, $\langle \cos \theta\_f \rangle$, and the fold–closure cross-correlation $\langle q\_f \cos \theta\_f \rangle$.

The results showed four robust qualitative features:

1. Fold order increased sharply above a threshold coupling region $J \sim 0.2$–0.25.
2. Closure coherence increased together with fold ordering — the two sectors did not transition independently.
3. Fold–closure alignment remained positive and strengthened with increasing fold order.
4. Closure-phase variance generally decreased as internal fold alignment increased.

The key structural result is therefore:

Fold criticality and closure coherence do not behave as independent sectors; they **co-organise dynamically** on the hexagonal-cell adjacency lattice.

The VERSF framework does not merely place folds and gauge transport on the same interface conceptually — the lattice computation suggests the same substrate dynamics drive both sectors toward ordered infrared structure simultaneously. This is early empirical support for the co-emergence picture that Conjecture 12.1 relies on.

Limitations. These calculations remain first-pass diagnostics rather than full lattice derivations: (1) the closure sector used compact face phases rather than the full link-based Wilson plaquette

structure of §12.12; (2) finite-size effects were not systematically analysed; (3) no continuum extrapolation was attempted; (4) the non-Abelian sectors of §12.11 were not included; (5) the fold-formation threshold operator $\Theta(\mathcal{C}\_\ell - \mathcal{C}^*)$ of §4.4 was approximated rather than dynamically evolved; (6) the measured effective couplings were obtained from simple correlation matching rather than the full inverse RG reconstruction of §12.12.

The natural next computational stages are full link-based Wilson closure transport on the hexagonal lattice; repeated block-fold RG iterations beyond single-step blocking; systematic finite-size scaling across multiple lattice sizes; explicit extraction of (ν, η, z, θ) from the stability matrix of §12.12; and the decisive test of §12.12 — whether a stable interacting closure fixed point with $\lambda \neq 0^*$ appears in the coupled system.

12.14 Open Programme for the Master Action

The eight concrete computational instances of §§12.6–12.13 identify the next steps for the master-action programme.

For §12.6 (block-fold RG flow): explicit computation of the partial trace on the hexagonal cell complex; determination of b_0 and η_fold from substrate dynamics; characterisation of the flow trajectories around $g^{*2} = 16\pi^2\,\eta\_\text{fold} / b_0$; computation of the leading scaling dimensions y_σ, y_ω at the fold critical points.

For §12.7 (critical exponents): refinement of the first-pass estimates (ν, η, z, θ, ζ, α) ≈ (1, 1/4, 2, −1, 1, −1) by computation of the corrections (δν_closure, δη_closure, δz_memory) from §12.6; sharper determination of θ from the bulk depth reconstruction (the present estimate θ ≈ −1 assumes exactly one reconstructed dimension at large scale); identification of subleading universality-class corrections from the coupling between Ising and gauge sectors.

For §§12.8–12.9 (closure-response kernel): derivation of λ_K from substrate dynamics rather than by Newtonian matching; extension of the conservation analysis beyond the flat low-curvature limit to a curved-background calculation with the full $\nabla\mu$ *commutator structure; characterisation of the spectral and propagation properties of* $K\{\mu\nu\}$ beyond the retarded prescription; integration with higher-derivative, massless, and anisotropic/saturation extensions.

For §12.10 (constrained uniqueness of the record-current functional): determination of the dimensional constants a, b from substrate-scale physics rather than empirical matching; explicit evaluation of the (K6) on-shell matching condition against the §10 / fold-density-gradients gravitational response, fixing the relation between ã and $\tilde{b}$ to a definite numerical value — framed as a joint calculation in Appendix A, with the substantive calculation slots identified there and completion identified as the natural next paper in the §12 strand; extension of the constrained-uniqueness analysis to subleading orders, deriving the coefficients of the parametrically suppressed (c, d, e, f, h) terms from substrate dynamics; and corpus-level order-matching of the leading-order linear-in-Φ result with the cubic-in-Φ structure expected of $\mathcal{S}$^μ — a consistency requirement on the TPB-entropy scaling, addressed elsewhere in the programme.

For §12.11 (non-Abelian closure): proof that admissibility, chirality, and closure sufficiency uniquely select the SU(3) × SU(2) × U(1) subgroup rather than merely allowing it; explicit construction of the structure constants f^a_{bc} from substrate dynamics; identification of the chirality-selection mechanism that promotes the structural decomposition to a true derivation.

For §§12.12–12.13 (lattice computation and diagnostics): extension of the §12.13 first-pass simulations to the full link-based Wilson plaquette structure of §12.12 (replacing the compact face-phase approximation); repeated block-fold RG iterations beyond the single-step blocking; systematic finite-size scaling across multiple lattice sizes; numerical extraction of (F_σ, F_ω, F_λ) by the full inverse RG reconstruction; measurement of the stability matrix eigenvalues and extraction of the critical exponents (ν, η, z) for direct comparison with the §12.7 analytic estimates; explicit dynamical evolution of the fold-formation threshold operator $\Theta(\mathcal{C}_\ell - \mathcal{C}^*)$; analysis of operator-basis truncation effects; and — the decisive question of §12.12 — resolution of whether a stable interacting fixed point with $\lambda \neq 0^*$ appears in the coupled system. The §12.13 finding that fold and closure sectors co-organise dynamically is encouraging but does not yet resolve the decisive test, which requires the full Wilson plaquette structure and multi-step RG iteration.

Beyond these per-section items, the broader master-action programme retains its central open targets: a proof that the four-fixed-point structure (Void, Fold, Maxwell, Einstein) closes (no competing fixed points); a treatment of the memory kernel under coarse-graining beyond the schematic $\zeta = 1$ form; and ultimately a rigorous proof of Conjecture 12.1 in its strengthened Yang–Mills form. Each is now a concrete technical question that the substrate-physics development of §§1–11 above, together with the calculational instances of §§12.6–12.13, can confront.

---

13. Conclusion: The Ontological Chain

The proposal of this paper is that the deepest physically active layer of reality in VERSF is the closure-bearing commitment interface separating reversible possibility from irreversibly committed structure. Every other physical structure in the framework can be located along the single ontological chain of Figure 1:

Void → Commitment Interface → Loops → Folds → Record → Gauge Transport → Geometry → Gravity → Effective Continuum Physics

Each link in this chain has been given a definite structural meaning. The Void is a constraint medium without operational structure, supporting no stable loops. The commitment interface is the minimal closure-bearing 2-surface on which $\beta_1 \geq 1$ becomes possible, with explicit interface cells $\varphi_i = (\sigma_i, \omega_i)$ and a transport action S_{int} combining nearest-neighbour transport, closure penalties, and a fold-formation threshold; each cell hosts a single fold whose per-fold Hilbert space is $\mathscr{H}_{\text{fold}} \cong \mathbb{C}^4$ in companion programme work. Loops are the non-contractible closure pathways enabled by this structure, and their formation is the trigger for fold formation. Folds — the first distinguishable asymmetries from the void — are the elementary irreversible

commitment events; their accumulation produces the record field ρ(x,t), whose monotonic growth supplies the framework's operational arrow of time. Gauge structure emerges as the interface's encoding redundancy modulo identical closure transport — formalised in Lemma 6.1 — with Wilson loops, holonomy, and F_μν all acquiring direct closure-theoretic meanings. Maxwell transport emerges as the continuum hydrodynamic limit of conserved closure transport — formalised in Lemma 7.2, Abelian in the present treatment — with the K = 7 constraint dimensionality and hexagonal tiling of the underlying admissibility architecture supplying the non-degenerate transport substrate. Geometry emerges as the bulk reconstruction of the accumulated record, and gravity as the Void's capacity response to its loading gradients.

What this paper actually does

The present paper does not claim a complete microscopic derivation of all physical structure from substrate dynamics alone. Its accomplishment is more specific.

It identifies a **common physical locus** for:

- fold formation,
- gauge transport,
- closure topology,
- record accumulation,
- geometric reconstruction,
- and gravitational response.

The proposal is that these structures are not independent layers of physics, but **different large-scale manifestations of the same underlying interface dynamics** populated by folds.

The master-action layer

Section 12 proposes that the substrate-structural development of §§3–10 supports a single candidate VERSF master action S_VERSF. Its constraint sector λ_μ(∇*v C^{μν} − 𝒮^μ) and matter coupling Φ*{μν}*𝒮*^{μν} together carry the closure dynamics of §§6–7 and the gravitational response of §10. §§12.1–12.5 state the programme structure (action, RG flow, fixed-point hierarchy, universality class, Conjecture 12.1); §§12.6–12.13 supply eight concrete computational instances, including an explicit block-fold RG flow with non-trivial gauge fixed point g² = 16π²η_fold/b₀, first-pass critical-exponent estimates, the conservation-fixed closure-response kernel K_{μν} = λ_K[m²g_{μν} G_m + ∇_μ∇ν G_m] mapping ρ → Φ{μν}, the constrained leading-order uniqueness theorem fixing C^{μν}[Φ] = aΦ^{μν} + bg^{μν}Φ (Theorem 12.2), the structural decomposition of SU(3) × SU(2) × U(1) from ℋ_fold ≅ ℂ⁴, an explicit Monte Carlo lattice programme, and first preliminary numerical diagnostics. The constitutive sector — the two functional inputs that distinguish the master action from a generic rank-2 EFT in curved spacetime (𝒮^{μν}[Φ] and C^{μν}[Φ]) — is now derived at leading order in functional form. Numerical content of the constitutive sector is the subject of Appendix A, which frames the joint calculation with §10 needed to reduce Theorem 12.2's two-parameter (a, b) family to a one-dimensional submanifold fixed by §10's calibration to Newton's G. The decisive $\lambda \neq 0$ lattice test of §12.12, the closure of the four-fixed-point structure of §12.3, and

subleading-order corrections beyond Theorem 12.2 remain open programme items, each addressed in its respective strand.

In this sense, the paper functions as a *unification layer* within the broader VERSF programme: not by replacing earlier transport and admissibility work, but by **locating where that physics physically lives**.

The broader significance is therefore the proposal that:

the deepest physically active layer of reality is an interface on which folds form — units of irreversible distinguishability that are the first asymmetries from the void.

The interface is *where reality becomes real*.

Appendix A: Framing for the Joint §10 ↔ §12.10 Matching Analysis

The (K6) matching condition of §12.10 — schematically $f(a, b) := \alpha b - \beta \cdot a \cdot \mathscr{R}[\Phi] = 0$ — is the further consistency requirement reducing the (a, b) plane to a one-dimensional submanifold, with explicit numerical content deferred to joint analysis with the §10 / fold-density-gradients construction. This appendix frames that joint analysis: the matching condition's structure (§A.1), the §10-side extraction (§A.2), the §12.10-side completion (§A.3), the matching that combines them (§A.4), and what the constitutive sector looks like once the joint calculation is complete (§A.5). The substantive numerical content — explicit forms for α and β in §10 variables and a leading-order substrate-scale value for $\mathscr{R}$ — is the subject of a forthcoming companion paper in the §12 programme strand. The framing here determines that paper's title, structure, methodology, and end-state: *The (K6) Matching Condition: Numerical Closure of the Record-Current Functional via the Rank-2 Gravitational Response.*

A.1 The matching condition: restatement

The conservation-constraint term in the VERSF master action is

$$S_C = \int d^4x \sqrt{(-g)}\, \lambda_\mu(\nabla_\nu C^{\mu\nu}[\Phi] - \mathcal{S}^\mu[\Phi]),$$

with $C^{\mu\nu}[\Phi]$ forced by Theorem 12.2 to the leading-order form $a\Phi^{\mu\nu} + bg^{\mu\nu}\Phi$. Substituting:

$$S_C = \int d^4x \sqrt{(-g)}\, \lambda_\mu(a\, \nabla_\nu \Phi^{\mu\nu} + b\, \nabla^\mu\Phi - \mathcal{S}^\mu).$$

The stress-energy contribution from variation with respect to $g^{\mu\nu}$ is $T^{(C)}_{\mu\nu} = (-2/\sqrt{(-g)})\, \delta S_C/\delta g^{\mu\nu}$. Three sources contribute: the $\sqrt{(-g)}$ measure, the Christoffel variation in ∇_ν acting on $\Phi^{\mu\nu}$, and the index-raising in $\nabla^\mu = g^{\mu\alpha}\, \nabla\alpha$. *Working through the*

standard variation (Christoffel variation, integration by parts, $\delta g^{\mu\nu} = -g^{\mu\alpha}g^{\nu\beta}\delta g_{\alpha\beta}$), the contribution decomposes into trace-free and trace tensor structures with coefficients linear in a and b respectively:

$$\mathbf{T^{(C)}_{\mu\nu}[\lambda, \Phi] = a \cdot \mathcal{T}^{(TF)}_{\mu\nu}[\lambda, \Phi] + b \cdot \mathcal{T}^{(Tr)}_{\mu\nu}[\lambda, \Phi] + (\text{metric-projected trace contributions}),}$$

where $\mathcal{T}^{(TF)}_{\mu\nu}$ *is symmetric and traceless and* $\mathcal{T}^{(Tr)}_{\mu\nu}$ carries the trace channel. The metric-projected trace contributions absorb the remaining terms into the trace channel without affecting the trace-free channel. The decomposition is unique for any symmetric rank-2 tensor; the trace-free and trace structures are linearly independent (neither transforms into the other by index relabelling or metric contraction), so a couples to the trace-free channel and b to the trace channel.

The independently derived rank-2 gravitational response of §10 supplies $T^{(\S10)}_{\mu\nu}$ via the fold-density-gradient construction. Writing the §10 response in the same trace-free / trace decomposition:

$$T^{(\S10,\,TF)}_{\mu\nu} = \alpha \cdot \mathcal{T}^{(TF,\,source)}_{\mu\nu}, \quad T^{(\S10,\,Tr)}_{\mu\nu} = \beta \cdot \mathcal{T}^{(Tr,\,source)}_{\mu\nu},$$

with α and β the trace-free and trace coefficients of the §10 response (definite expressions in the §10 variables — developed in §A.2), constraint (K6) requires consistency between $T^{(C)}$ and $T^{(\S10)}$ at the matching level. Reducing the pair of channel-by-channel matching conditions to a single algebraic relation:

$$\mathbf{f(a, b) := \alpha\, b - \beta \cdot a \cdot \mathscr{R} = 0,}$$

where $\mathscr{R}$ is the leading-order substrate-scale ratio between the on-shell trace and trace-free constraint-sector channels (developed in §A.3). The schematic $\mathscr{R}[\Phi]$ notation of §12.10 reflects the fact that $\mathscr{R}$ acquires Φ-dependence at sub-leading orders through EFT-suppressed corrections; at the order Theorem 12.2 operates, $\mathscr{R}$ is a substrate-scale constant rather than a Φ-dependent functional. This is the (K6) matching condition in the form stated in §12.10. The remainder of this appendix frames the joint calculation that supplies the explicit forms of α, β, and $\mathscr{R}$.

A.2 The §10 extraction

The §10 extraction develops three pieces: the §10 gravitational response in its native variables, the change of basis into the $(\mathcal{T}^{(TF)}, \mathcal{T}^{(Tr)})$ tensor decomposition, and the explicit identification of α and β as functions of the §10 variables. A fourth piece — on-shell linear independence — is structural rather than computational.

The §10 response in its native variables. The §10 / fold-density-gradients construction supplies the rank-2 gravitational response $T^{(\S10)}_{\mu\nu}$ *in its own native variables: the rank-2 commitment field* $\Phi_{\mu\nu}$ built from the scalar record density ρ via the closure-response kernel of §§12.8–12.9, the fold density structure, and the curvature scale fixed by Newton's G. What the

joint calculation draws from §10 is the explicit functional form of $T^{(\S10)}_{\mu\nu}[\Phi, \rho, \nabla]$ in the trace-free and trace channels, with dimensionful coefficients expressed in terms of fold-density-gradient parameters and the geometric calibration to Newton's G.

Change of basis. The §10 response is decomposed into trace-free and trace parts and expressed in terms of the source tensor structures $\mathcal{T}^{(TF, source)}$ and $\mathcal{T}^{(Tr, source)}$ of §A.1. The trace-free channel of $T^{(\S10)}$ carries the anisotropic record content — sourcing gravitational tensor modes and anisotropic stress; the trace channel carries the conformal record content — scale-dependent, directionally isotropic.

Identification of α and β. With the §10 response written in the source basis, the coefficients α and β are read off directly:

α = trace-free coefficient of $T^{(\S10)}$ in the source basis, β = trace coefficient of $T^{(\S10)}$ in the source basis.

Both are dimensionful substrate-scale quantities, fixed by the §10 calibration to Newton's G and to the fold-density-gradient structure. Their explicit forms in terms of §10 variables are the substantive content of the §10 extraction.

On-shell non-degeneracy (structural). The trace-free and trace channels are linearly independent at the tensor level *by construction of the trace decomposition*: $\mathcal{T}^{(TF)}_{\mu\nu}$ *is traceless and* $\mathcal{T}^{(Tr)}_{\mu\nu}$ is pure-trace, so no index relabelling or metric contraction transforms one into the other. The matching condition's non-degeneracy is therefore not at risk from generic on-shell evaluation. The only way it could collapse is if the master action's equations of motion forced $\Phi_{\mu\nu}$ into a pure-trace configuration ($\Phi_{\mu\nu} \propto g_{\mu\nu}$), which would contradict the non-degeneracy already established in Theorem 10.0 of §10. The on-shell non-degeneracy of the matching is therefore a *structural consequence* of the trace decomposition together with Theorem 10.0, not a calculation that needs separate verification.

The output of §A.2 is a pair of definite expressions for α and β in terms of §10 variables, with on-shell non-degeneracy guaranteed structurally.

A.3 The §12.10 completion

The §12.10 completion develops three pieces: the variational calculation of $T^{(C)}_{\mu\nu}$ carried out in full rather than schematically, the on-shell evaluation of the resulting tensors on the master action's field equations, and the resulting leading-order substrate-scale constant $\mathscr{R}$.

The constraint-sector variation, completely. The variation of the constraint sector S_C with respect to $g^{\mu\nu}$ is carried out term by term: each Christoffel contribution is expanded and integrated by parts to move derivatives off $\delta g^{\mu\nu}$, with boundary terms discarded under asymptotic falloff (or compact support of test configurations). The resulting expressions for $\mathcal{T}^{(TF)}_{\mu\nu}[\lambda, \Phi]$ *and* $\mathcal{T}^{(Tr)}_{\mu\nu}[\lambda, \Phi]$ are explicit local tensor expressions in λ, Φ, and their covariant derivatives — symmetric in (μν), at most second order in covariant derivatives, consistent with the leading-order EFT power-counting of §12.10.

On-shell evaluation. The leading-order substrate-scale constant $\mathscr{R}$ entering the matching condition arises from on-shell evaluation of the constraint-sector tensors. The on-shell configurations are determined by:

- The variational equation for λ_μ: ∇_ν C^{μν} = $\mathcal{S}$^μ (the conservation identity itself).
- The variational equation for Φ_{μν}: contributions from kinetic, mass, matter-coupling, and constraint-sector λ_μ-coupling.
- The variational equation for the metric: the full stress-energy balance, with T^{(C)} entering as one contribution.

The on-shell evaluation of $\mathcal{T}$^{(TF)}[λ, Φ] and $\mathcal{T}$^{(Tr)}[λ, Φ] is carried out by substitution in the regime where the master action's leading-order EFT power-counting applies. The on-shell λ_μ is determined by the conservation identity and the matter-coupling structure; the on-shell Φ_{μν} is determined by its field equation in the absence of higher-derivative or curvature-coupled corrections.

The leading-order ratio $\mathscr{R}$. $\mathscr{R}$ is defined as the relative scaling between the trace-free and trace channels of T^{(C)} on-shell:

$\mathscr{R}$:= (trace-channel coefficient of T^{(C)}*{on-shell}) / (trace-free-channel coefficient of T^{(C)}*{on-shell}),

with the proportionality constants set by the source tensors $\mathcal{T}$^{(TF, source)} and $\mathcal{T}$^{(Tr, source)} of §A.1. In the leading-order regime — the regime in which Theorem 12.2 operates and the matching condition is applied — $\mathscr{R}$ reduces to a substrate-scale constant determined by Φ_sub, Λ_sub, ℓ_sub, and the §10 calibration. Φ-dependence enters at sub-leading orders through EFT-suppressed corrections in the on-shell evaluation; at the order Theorem 12.2 operates, $\mathscr{R}$ is a finite substrate-scale number, and its calculation reduces to a finite-dimensional substrate-scale determination rather than an evaluation of a functional.

The output of §A.3 is a definite leading-order substrate-scale value for $\mathscr{R}$.

A.4 The matching

With α, β from §10 (§A.2) and the leading-order constant $\mathscr{R}$ from the §12.10 completion (§A.3), the matching condition f(a, b) := α b − β · a · $\mathscr{R}$ = 0 reduces from schematic relation to definite algebraic constraint:

α · b − β · a · $\mathscr{R}$ = 0 ⟺ b/a = (β · $\mathscr{R}$) / α.

Both α and β are dimensionful substrate-scale coefficients of the §10 response; $\mathscr{R}$ is the leading-order substrate-scale ratio. Their combination (β · $\mathscr{R}$) / α is a definite substrate-scale ratio, fixed by the §10 calibration. The expected qualitative properties: the ratio is positive (the trace-free and trace channels carry record-content of the same sign in the leading-order regime — a consequence of the on-shell non-degeneracy structurally established in §A.2) and of order unity (no large hierarchy between trace-free and trace channels at leading order).

Reduction to a one-dimensional submanifold. The matching condition fixes the ratio of trace-free and trace coefficients in the original (a, b) parameterisation. In the trace / trace-free decomposition of §12.10 — C^{μν} = ã(Φ^{μν} − ¼g^{μν}Φ) + b̃g^{μν}Φ with ã = a, b̃ = a/4 + b — the constraint takes the form

$\tilde{b}/\tilde{a} = ¼ + (\beta \cdot \mathscr{R}) / \alpha.$

The two-parameter (a, b) plane reduces to a one-dimensional submanifold parameterised by a single overall scale.

Natural normalisation. The remaining single overall scale corresponds to the dimensional normalisation of the record-current functional itself. The §10 construction fixes Newton's G in terms of substrate-scale quantities via the fold-density-gradient gravity structure; carrying this calibration through to the record-current normalisation gives a definite substrate-scale value for a and — via the matching ratio — for b. The result: both a and b are fixed in substrate-scale units up to a choice of geometric convention (overall sign and units of the Φ field). These conventions are the standard residual freedom in any variational formulation; they do not represent undetermined physics.

A.5 What completing this analysis would accomplish

Three substantive consequences follow once the joint calculation is complete.

Caveat (ii) of §12.10 is retired to one-parameter level. §12.10 currently states: "*(ii) The dimensional constants a, b are forced to be substrate-scale but are not derived from first principles — their values require additional substrate-level analysis or empirical matching.*" After the joint analysis: a and b are no longer independent (their ratio fixed by the (K6) matching); the remaining single overall scale is fixed by §10 calibration against Newton's G; the residual freedom is convention-level (units, sign), not physics-level. The caveat does not entirely vanish — a, b are not derived from a deeper first-principles substrate dynamics, only from the §10 calibration, which is itself a derived structure elsewhere in the programme. The chain of derivation has lengthened by one step and the underived input has moved upstream rather than disappeared. This is the correct epistemic position: the constitutive sector is closed at leading order up to inputs that are themselves derived elsewhere.

The constitutive sector of the master action is derived rather than postulated. The two functional inputs distinguishing the VERSF master action from a generic rank-2 EFT in curved spacetime — the commitment-density functional $\mathcal{S}^{μν}[Φ]$ (closed by the TPB-entropy structure of the programme work) and the record-current functional C^{μν}[Φ] (closed at leading order by Theorem 12.2 here together with the (K6) matching) — are both derived at leading order. The remaining content of the master action (kinetic, mass, Einstein–Hilbert) is inherited from the standard variational form for rank-2 tensor matter in curved spacetime; no further constitutive input is required.

Conjecture 12.1 strengthens further. §12.10 already upgraded Conjecture 12.1's strengthened form from "a family indexed by free constitutive functionals" to "a single specific theory rather

than a family." Completion of the joint analysis upgrades further to "a single specific theory up to convention" — the same theoretical commitment, now with numerical content as well as functional form fixed at leading order.

What remains open. Three items from §12.10 caveat (iii), plus the TPB order-matching, remain open: (i) the decisive $\lambda^* \neq 0$ lattice test of §12.12; (ii) the closure of the four-fixed-point structure of §12.3; (iii) subleading corrections to $C^{\{\mu\nu\}}[\Phi]$ from the parametrically suppressed coefficients (c, d, e, f, h) of §12.10's candidate space; and (iv) the corpus-level order-matching $TPB[\Phi] \sim |\Phi|^2$ consistency requirement, addressed by the TPB-entropy programme work. These are separate research strands, each addressed in its own part of the programme.

A.6 Programme of the joint analysis

The substantive content of the joint §10 ↔ §12.10 analysis is summarised below:

- **§A.2 (§10 extraction).** The §10 gravitational response in its native variables; change of basis into the $(\mathcal{T}^{(TF)}, \mathcal{T}^{(Tr)})$ decomposition; explicit identification of α and β as expressions in §10 variables. On-shell non-degeneracy of the matching is a structural consequence of the trace decomposition together with Theorem 10.0, not an independent calculation.
- **§A.3 (§12.10 completion).** Full variational calculation of $T^{(C)}_{\mu\nu}$ completing the schematic of §12.10; on-shell evaluation of the constraint-sector tensors on the master action's field equations; leading-order substrate-scale value for $\mathscr{R}$ (a finite substrate-scale determination, not a Φ-dependent functional evaluation).
- **§A.4 (the matching).** Numerical reduction of $f(a, b) = 0$ with α, β, $\mathscr{R}$ inserted; normalisation against Newton's G via the §10 calibration.

The framing of each section identifies what enters, what is computed, and what comes out. The substantive completion of each section is the content of the forthcoming companion paper in the §12 programme strand.

References

VERSF programme works

The present paper is part of a multi-paper VERSF programme developed by the author at the AIDA Institute (versf-eos.com). Companion programme works referenced throughout — on the substrate physics of the commitment interface, the per-fold Hilbert structure, the K = 7 admissibility architecture, hexagonal interface light propagation, the emergent depth axis, the tick–bit asymmetry, the synthesis-paper derivation of the Standard Model gauge group, the gravity-sector papers (tensorial closure of record dynamics, coherence scale and memory kernel, fold density gradients, critical entropic back-pressure, bit conservation), the BCB–VERSF hierarchical clarification, physical admissibility, the non-Abelian gauge algebra and chirality

selection, and the programme overview — are catalogued at the programme website and in the *Guide to VERSF* (versf-eos.com / AIDA Institute).

Standard literature

- Adler, S. L. (1995). *Quaternionic Quantum Mechanics and Quantum Fields.* Oxford University Press.
- Ashkin, J. & Teller, E. (1943). Statistics of two-dimensional lattices with four components. *Physical Review* **64**(5–6), 178–184.
- Bekenstein, J. D. (1973). Black holes and entropy. *Physical Review D* **7**(8), 2333–2346.
- Bennett, C. H. (1982). The thermodynamics of computation — a review. *International Journal of Theoretical Physics* **21**(12), 905–940.
- Bombelli, L., Lee, J., Meyer, D., & Sorkin, R. D. (1987). Space-time as a causal set. *Physical Review Letters* **59**(5), 521–524.
- Burgess, C. P. (2007). Introduction to effective field theory. *Annual Review of Nuclear and Particle Science* **57**, 329–362.
- Donoghue, J. F. (1994). General relativity as an effective field theory: The leading quantum corrections. *Physical Review D* **50**(6), 3874–3888.
- Hales, T. C. (2001). The honeycomb conjecture. *Discrete & Computational Geometry* **25**(1), 1–22.
- Hatcher, A. (2002). *Algebraic Topology.* Cambridge University Press.
- Hawking, S. W. (1975). Particle creation by black holes. *Communications in Mathematical Physics* **43**(3), 199–220.
- Jacobson, T. (1995). Thermodynamics of spacetime: The Einstein equation of state. *Physical Review Letters* **75**(7), 1260–1263. arXiv:gr-qc/9504004.
- Kadanoff, L. P. (1966). Scaling laws for Ising models near T_c. *Physics Physique Fizika* **2**(6), 263–272.
- Kogut, J. & Susskind, L. (1975). Hamiltonian formulation of Wilson's lattice gauge theories. *Physical Review D* **11**(2), 395–408.
- Landauer, R. (1961). Irreversibility and heat generation in the computing process. *IBM Journal of Research and Development* **5**(3), 183–191.
- Lovelock, D. (1971). The Einstein tensor and its generalizations. *Journal of Mathematical Physics* **12**(3), 498–501.
- Maxwell, J. C. (1865). A dynamical theory of the electromagnetic field. *Philosophical Transactions of the Royal Society of London* **155**, 459–512.
- Onsager, L. (1944). Crystal statistics. I. A two-dimensional model with an order-disorder transition. *Physical Review* **65**(3–4), 117–149.
- Renou, M.-O., Trillo, D., Weilenmann, M., Le, T. P., Tavakoli, A., Gisin, N., Acín, A., & Navascués, M. (2022). Quantum theory based on real numbers can be experimentally falsified. *Nature* **600**, 625–629.
- Susskind, L. (1995). The world as a hologram. *Journal of Mathematical Physics* **36**(11), 6377–6396. arXiv:hep-th/9409089.
- 't Hooft, G. (1993). Dimensional reduction in quantum gravity. arXiv:gr-qc/9310026.
- Verlinde, E. (2011). On the origin of gravity and the laws of Newton. *Journal of High Energy Physics* **2011**(04), 029. arXiv:1001.0785.
- Weinberg, S. (1995). *The Quantum Theory of Fields*, vol. I. Cambridge University Press.

- Weinberg, S. (2016). Effective field theory, past and future. *International Journal of Modern Physics A* **31**(6), 1630007.
- Wheeler, J. A. (1990). Information, physics, quantum: The search for links. In W. H. Zurek (ed.), *Complexity, Entropy, and the Physics of Information*. Addison-Wesley.
- Wilson, K. G. (1974). Confinement of quarks. *Physical Review D* **10**(8), 2445–2459.
- Wilson, K. G. & Fisher, M. E. (1972). Critical exponents in 3.99 dimensions. *Physical Review Letters* **28**(4), 240–243.
- Yang, C. N. & Mills, R. L. (1954). Conservation of isotopic spin and isotopic gauge invariance. *Physical Review* **96**(1), 191–195.